# A CONNECTION BETWEEN ANALYTIC AND NONANALYTIC SINGULAR PERTURBATIONS OF THE QUADRATIC MAP

A THESIS
SUBMITTED TO THE FACULTY OF THE GRADUATE SCHOOL
OF THE UNIVERSITY OF MINNESOTA
BY

YUJIONG LIU

IN PARTIAL FULFILLMENT OF THE REQUIREMENTS
FOR THE DEGREE OF
MASTER OF SCIENCE

ADVISOR: BRUCE PECKHAM

MAY, 2017

# Acknowledgements

In this research, there are many people I should express my gratitude to. The first one is my advisor, Professor Bruce Peckham. It is his passion and patient guidance that attract me to step into this fantastic area. He is such a good advisor that when I am stuck at some spot, he likes to help me to go back and review my thoughts and when I made some progress, he encourages me to go further. I would also like to thank Professor Marshall Hampton and Professor Douglas Dunham for serving on my committee, examining my report and hearing my defense. Finally, I must express my deepest gratitude to my parents. I could not accomplish any of my work without their unfailing support.

## Abstract

To explore the connection between the analytic and the nonanalytic complex dynamics, this paper studied a special case of the singularly perturbed quadratic map:

$$f_{\beta,t}(z) = z^2 + t\frac{\beta}{z^2} + (1-t)\frac{\beta}{\bar{z}^2}$$

which can transit from nonanalytic to analytic by varying $t$ from 0 to 1. Other variables involved in this map are the dynamic variable $z \in \mathbb{C}$ and the main parameter $\beta \in \mathbb{R}$. Our investigation shows that this transition map has much richer behaviors than the end point cases. The parameter space can be no longer subdivided into only four or three regions as shown in the studies by Devaney and Bozyk respectively. Correspondingly, in the dynamic plane, there also appear several new intermediate cases among which we identified two transitions: a connected case where the filled Julia set is connected and a disconnected case where the filled Julia set consists of infinitely many components. This paper also pointed out that $f_{\beta,t}(z)$ is semiconjugate to the four symbols shift map for the disconnected case. This semiconjugacy provides a way to largely understand the dynamical behaviors for the non escape points. Further study shows that the critical set plays an important role in the construction of the filled Julia set. Therefore, the transition of the critical set and its image set are also discussed in this paper. At the end, we presented two sets of conjectures for the bounded critical orbits and the escape critical orbits for future study.

# Contents

# List of Figures

# Chapter 1

# Introduction

## 1.1 Background and Research Goals

The start of complex dynamics can trace back to 100 years ago[1], as Gaston Julia and Pierre Fatou won the 1918 Grand Prize. Their main contributions were introducing the normal family theory developed by Paul Montel into complex dynamics research. This powerful tool provides a new viewpoint of the iteration procedure and therefore divides the whole dynamic space into two categories. One is the so-called Julia set and the other is the Fatou set. Intuitively, the Fatou set are all the points whose behaviors are regular, or the points on which the iteration function family constitutes a normal family[2]. The Julia set consists of the points whose behaviors are irregular. Obviously, the Julia set is the complement of the Fatou set. This fundamental division turns out to be very useful and insightful to understand the global behaviors of a complex map.

However, after Julia and Fatou solved the open question for the Grand Prize, there was little progress in this area until the late 1970s, when Benoit Mandelbrot[3] generated a fractal in the parameter plane by using the emerging computer technology. This set is now named the Mandelbrot set after its discoverer. These fractal pictures are so beautiful and interesting that many mathematicians were attracted to work on this area. Since then, much significant progress has been made, and the area has produced several Fields medalists, including John Milnor[4], whose book serves as the main reference for the classical complex dynamics in this paper.

Classical complex dynamics mainly talks about the general properties of complex one-dimensional rational maps. Complete understanding of rational maps is a challenging goal. Therefore, from 2002, Robert Devaney[5, 6] started to work on a special category of rational maps, the singular perturbations of the quadratic family. These maps have some behaviors similar to the well-known quadratic family but they also have many special characteristics brought by the singular perturbation term, such as the trap door, the Sierpinski carpet[7, 8, 9] structure and the McMullen domain[10].

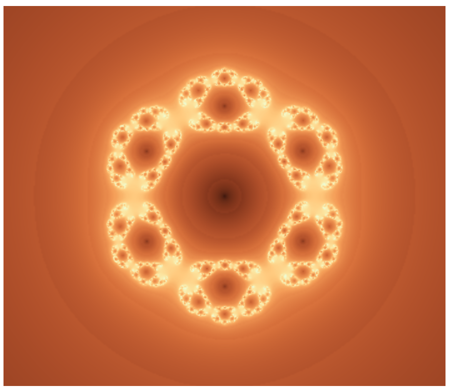

(a) Julia set is a Cantor set ($\lambda = 0.175$)

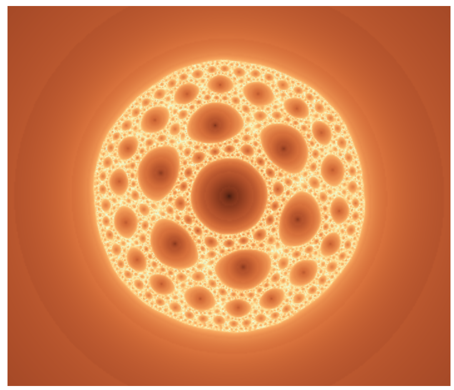

(b) Julia set is a Sierpinski carpet ($\lambda = 0.03 - 0.03i$)

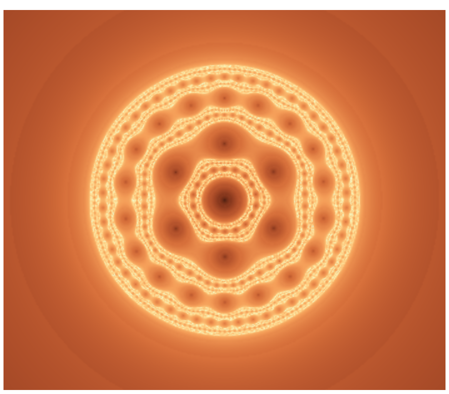

(c) Julia set is a Cantor set of circles ($\lambda = 0.007$ which is in the McMullen domain)

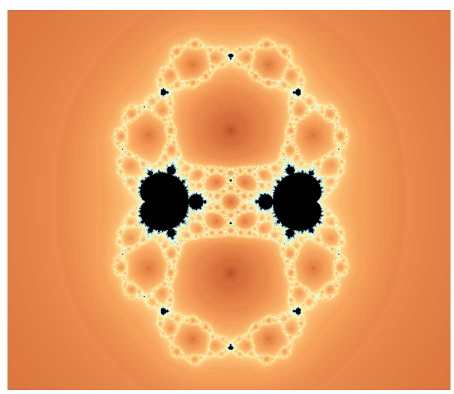

(d) The $\lambda$ parameter plane

Figure 1.1: The escape trichotomy for the map $f(z) = z^3 + \frac{\lambda}{z^3}$

He also expanded his study scope from quadratic maps to higher degree maps.

$$z^2 + \frac{\epsilon}{z} \to z^2 + \frac{\lambda}{z^2} \to z^n + \frac{\lambda}{z^m}$$

in which $\epsilon \in \mathbb{R}^+$, $\lambda \in \mathbb{C}$, $m, n \in \mathbb{Z}$. Note that the right arrows in this expression just mean the evolution of the iteration formulas.

Devaney's research shows that the behavior of critical orbits can determine a surprising amount of information about the iteration map. One such result is the escape trichotomy[11]. See section 1.2 for notation and definitions.

**Theorem.** *Let $F_\lambda(z) = z^n + \frac{\lambda}{z^n}$ and suppose the orbits of the free critical points tend to $\infty$*

(1) *If $\upsilon_\lambda$ lies in $B_\lambda$, the $J(F_\lambda)$ is a Cantor set.*

(2) *If $\upsilon_\lambda$ lies in $T_\lambda$, the $J(F_\lambda)$ is a Cantor set of concentric simple closed curves, each one of which surrounds the origin. All $\lambda$s belonging to this case constitute the so-called McMullen domain.*

(3) *In all other cases, $J(F_\lambda)$ is a connected set, and if $F_\lambda^k(\upsilon_\lambda) \in T_\lambda$ where $k \geq 1$, then $J(F_\lambda)$ is a Sierpiński curve.*

Fig 1.1 shows these three typical Julia sets and the corresponding parameter set.

Although Devaney's research is excellent, his theorem can not be generalized to nonanalytic maps. Actually, many of the theorems from the classical complex dynamics will fail for the nonanalytic case. One reason is because nonanalytic maps no longer have a complex derivative and then have critical curves instead of isolated critical points, which makes the mapping properties extremely complicated. Therefore, for the nonanalytic case, people were trying to find out other tools to investigate this case and understand its dynamical behaviors.

One early such trial was done by Bruce Peckham[12] in 1998. In this research, he investigated the bifurcation properties of the map $f(z) = z^2 + C + \alpha\overline{z}$ and identified the evolution of "Arnold tongues" from bulb tangency points in the Mandelbrot set as $\alpha$ transitions from zero to nonzero.

Another related trial was on an angle-doubling map which has the iteration formula $f(z) = (1 - \lambda + \lambda|z|^2)(\frac{z}{|z|})^2 + c$. This case was explored by Stefanie Hittmeyer, Bernd

Krauskopf and Hinke Osinga[13] in 2015. The advantage of this map is that it can go from the standard analytic quadratic map to nonanalytic angle-doubling map by varying $\lambda$ from 1 to 0.

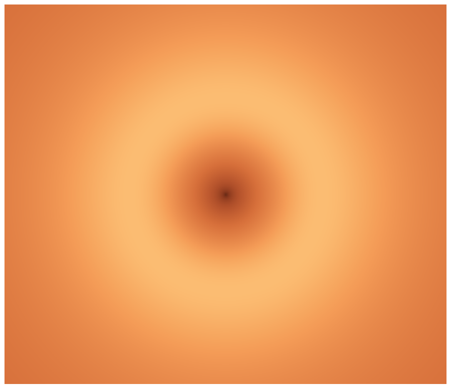

(a) Filled Julia set is empty ($\beta = 0.25$)

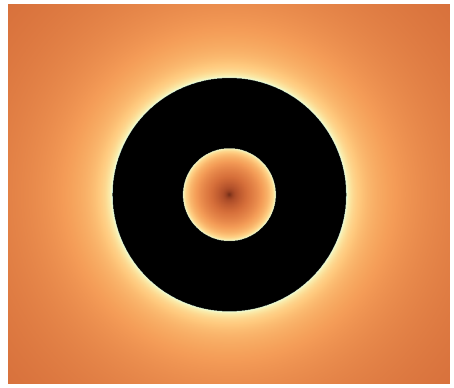

(b) Filled Julia set is an annulus ($\beta = 0.08$)

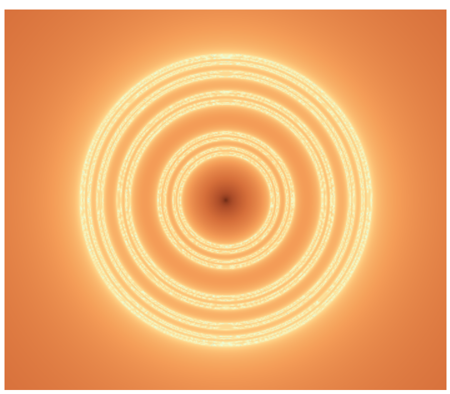

(c) Filled Julia set is a Cantor set of circles ($\beta = -0.09 - 0.09i$ which is in the McMullen domain)

(d) The $\beta$ parameter plane

Figure 1.2: The different dynamical behaviors of the map $f(z) = z^3 + \frac{\beta}{\bar{z}^3}$

In 2013, Brett Bozyk and Bruce Peckham[14] studied an even nicer nonanalytic iteration map $f(z) = z^n + \frac{\beta}{\bar{z}^n}$. This formula has a very good property: the radius can be decoupled from the angle (but the angle is still related to the radius). This property actually reduced the original map down to a one dimensional "radius" map. The three different classes of filled Julia sets as well as the parameter plane for this family are shown in fig 1.2.

Since the analytic and the nonanalytic perturbations have many different characters, we are curious about what happens during the transition between these two cases. Thus we developed a new iteration formula which enables the perturbation to go from nonanalytic to analytic. Here is the function:

$$f(z) = z^n + t\frac{\alpha}{z^{d_1}} + (1-t)\frac{\beta}{\overline{z}^{d_2}}$$

where $t$ is a real number from 0 to 1, $n$, $d_1$, $d_2$ are positive integer, $\alpha$, $\beta$ are parameters.

For simplicity, this paper will just focus on the case when $\alpha = \beta \in R$ and $n = d_1 = d_2 = 2$

$$f_{\beta,t}(z) = z^2 + t\frac{\beta}{z^2} + (1-t)\frac{\beta}{\overline{z}^2} \tag{1.1}$$

Note that fig 1.1 and 1.2 were for $n = d_1 = d_2 = 3$. This is similar to the figures for $n = d_1 = d_2 = 2$ except that in the complex analytic case, there is no McMullen domain.

Therefore, our main goal in this paper is to find out how the dynamical behavior of $f$ changes as the map goes from analytic to nonanalytic, more specifically, as $t$ goes from 1 to 0. Further, we would like to find out the connection between these changes and the critical set escape properties. These preliminary explorations will help us to better understand the roles that the critial set plays on the dynamical behaviors.

Here are the arrangements and contents of each chapter.

- Chapter 2 briefly presents the dynamical behaviors of $f$ restricted to the reals. Research on this case turns out to be very useful in the more general case: $z \in \mathbb{C}$.

- In Chapter 3 the critical set of $f$ and its images are computed. We also found the analytic expression of the critical set by using the "$z - \overline{z}$ coodinates". Based on this fact, the transition of the critical set and its images are also explored in this chapter.

- Chapter 4 describes the filled Julia set of $f$ and some of its connections with the critical set. Several preliminary results as well as conjectures are given in this chapter.

- Chapter 5 summarizes this main points in this paper.

## 1.2 Definitions and Notation

Since the notation below and terminology keep appearing in this paper, we define these terms first.

1. $O^+(z)$, $O^-(z)$: the images and preimages of $z$. These images and preimages consititute the so called forward and backward orbits of $z$.

2. $A(z)$: all points whose orbits go to $z$ eventually. This is always called the basin of attraction of $z$.

3. $B(\infty)$: the connected component of $A(\infty)$ containing $\infty$. This is always called the immediate basin of attraction of $\infty$.

4. $T(f)$: the preimage of $B(\infty)$ other than itself when $0 \notin B(\infty)$. This is the so-called trap door which normally resides in a neighborhood of the singularity (at $z = 0$).

5. $C(f)$: this is the critical set of $f(z)$ which has several different definitions. One of these definitions, probably the most insightful one, is the set of points whose local injective property fails. Although this definition is nice, it is actually hard to use. So people also developed several equivalent definitions for different maps. For instance, if $f(z)$ is a complex rational map, then the critical points are defined by $\{z \in \mathbb{C} | f'(z) = 0\}$. If $f(x, y)$ is a two dimensional real map, the critical set is defined by $\{(x, y) \in \mathbb{R}^2 | Det(J) = 0\}$ where $Det(J)$ is the determinant of the Jacobian matrix at this point. Since our map $f(z)$ is nonanalytic, we use this last definition. The critical set is also denoted by $J_0$ referring to the Jacobian matrix.

6. $V(f)$: the image of $C(f)$, also denoted by $J_1$.

7. Free critical points: all critial points other than 0 and $\infty$ are called free critical points ($\infty$ is always a critical point).

8. Prepole: the preimages of 0.

9. $K(f)$: all the points staying bounded. This is always called the filled Julia set.

10. $J(f)$: the Julia set of $f(z)$. There are also many different but equivalent definitions for this set in the complex analytic case. For instance, the Julia set is all the points on which $f(z)$ is not normal, or the set consisting of the closure of all the repelling periodic points. In our case, for simplicity, we use another equivalent definition: Julia set is the boundary of the filled Julia set.

11. $F(f)$: for complex analytic maps, the set on which $f(z)$ is normal or the complement of the Julia set $J(f)$. This is also called the Fatou set.

12. $z-\overline{z}$ coordinates: $f(z)$ can be also interpreted as a map in $\mathbb{R}^2$ with the constraint of $\overline{z}$ being the conjugate of $z$. This is the so-called $z-\overline{z}$ coordinates. By using this coordinate system, $f(z)$ can be written as $f_{\beta,t}(z,\overline{z})$.

13. Complex analytic versus complex in $z-\overline{z}$: the first term mainly refers to a complex analytic map in the complex plane, while the second is just a convenient way of expresssing a map in $\mathbb{R}^2$.

# Chapter 2

# Dynamics on the Real Axis

One benefit of the simplified iteration formula (1.1) is that when $\beta$ is real, the real axis is invariant. Further, when we restrict $z$ on real axis, $t$ can be cancelled. Let

$$z = x + iy$$

$$\overline{z} = x - iy$$

then $y = 0$ implies $z = x$ and $\overline{z} = x$. So

$$\begin{aligned} f(x) =& x^2 + t\frac{\beta}{x^2} + (1-t)\frac{\beta}{x^2} \\ =& x^2 + \frac{\beta}{x^2} \end{aligned} \tag{2.1}$$

which means the dynamical behavior of (1.1) on the real axis is not affected by t. This nice property allows us to explore some one-dimensional real dynamics before fully getting into the complex plane.

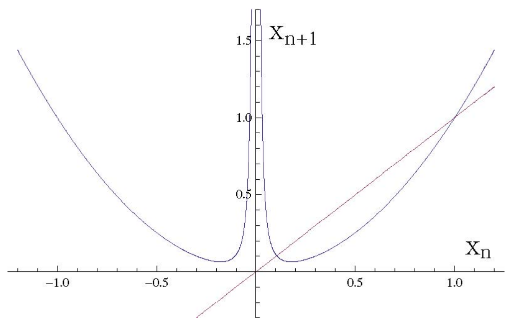


Figure 2.1: Graph of $x_{n+1} = x_n^2 + \frac{0.001}{x_n^2}$ and the reference line $x_{n+1} = x_n$

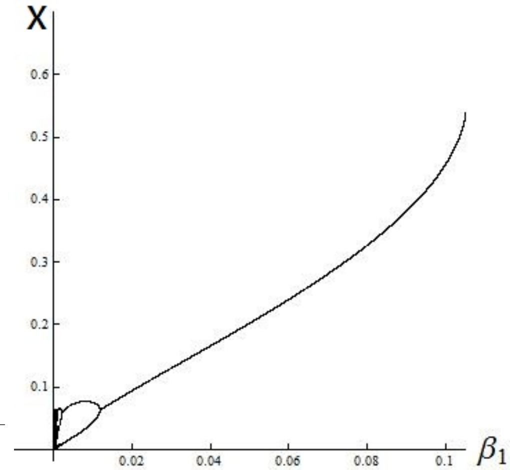


Figure 2.2: Orbit diagram of equation (2.1) for real $\beta$

## 2.1 Fixed Points

Fig. 2.1 is the graph of the iteration function in (2.1) when $\beta = 0.001$. From this graph, we find that there are two fixed points. They satisfy this equation

$$x^4 - x^3 + \beta == 0 \tag{2.2}$$

Since it is hard to write down the analytic solutions of this equation, we will mainly use numerical results to handle further computations. When $\beta = 0.001$, the two fixed points are approximately

$$x_1 = 0.103717, \quad x_2 = 0.998997$$

After finding the fixed points, naturally, we would like to know their stability. Therefore, compute the derivative function first

$$f'(x) = 2x - 2\beta x^{-3} \tag{2.3}$$

Then plug these two fixed points into (2.3)

$$f'(x_1) \approx -1.6 < -1, \quad f'(x_2) \approx 2 > 1$$

This means these two fixed points are both repelling.

## 2.2 Bifurcation Points as $\beta$ Varies

Plug (2.2) into (2.3)

$$f'(x) = 4x - 2 \tag{2.4}$$

This is the derivative at the fixed points. To solve for the transition between attracting and repelling, we let (2.4) equal to 1 and $-1$ to find out the corresponding roots. Then substitute these roots back to (2.2) to get the Saddle-Node bifurcation point and Period-Doubling bifurcation point

$$\textit{Saddle node}:\ b_1 = \frac{27}{256},\ \textit{Period doubling}:\ b_2 = \frac{3}{256} > 0.001$$

Since higher period bifurcations are hard to compute analytically, we used TBC software (see appendix A) to explore the higher period orbits. It turned out the only attracting cycle when $\beta = 0.001$ is 8. The full orbit diagram is shown in fig 2.2. Note that this diagram is a full diagram although it seems truncated. More details about this phenomenon can be found in [14] and in Devaney's work [15].

## 2.3 More Discussion

From both Devaney's and Bozyk's work, $n = 2$ is a special case. For Devaney's case (analytic), the special part is that there is no McMullen domain in the parameter plane. But for Bozyk's case (nonanalytic), the special part is that the orbit diagram for real $\beta$ is no longer a "full family" (refer fig 2.2). It turns out that both of these characteristics are determined by the critical orbit behavior, more specifically, whether the critical orbit goes into the trap door or not. So in this section, we would like to verify these characteristics just from the real axis.

At first, by letting function (2.3) equal to 0, we can find the critial points

$$C(f(x)) = \pm\sqrt[4]{\beta}$$

Then the start of the critical orbit can be computed

$$\pm\sqrt[4]{\beta} \to 2\sqrt{\beta} \to 4\beta + \frac{1}{4}$$

We then define two functions $s(x)$ and $k(x)$

$$
\begin{aligned}
s(x) =& f(x) - x \\
=& x^2 + \frac{\beta}{x^2} - x \\
=& \frac{x^4 - x^3 + \beta}{x^2} \\
=& \frac{k(x)}{x^2}
\end{aligned}
\tag{2.5}
$$

It is easy to see that when $x > 0$, $s(x)$ and $k(x)$ have the same signs. Actually, $k(x)$ represents the relationship between $f(x)$ and the reference line. If $k(x) > 0$, $f(x)$ is above the reference line; if $k(x) < 0$, $f(x)$ is below the reference line; if $k(x) = 0$, $f(x)$ is a fixed point. Based on this observation, evaluate $k(4\beta + \frac{1}{4})$ to decide if $4\beta + \frac{1}{4}$ could be above the reference line.

$$
k(4\beta + \frac{1}{4}) = 256\beta^4 - 6\beta^2 + \frac{\beta}{2} - \frac{3}{256}
$$

Then plot $k(4\beta + \frac{1}{4})$ respect to $\beta$.

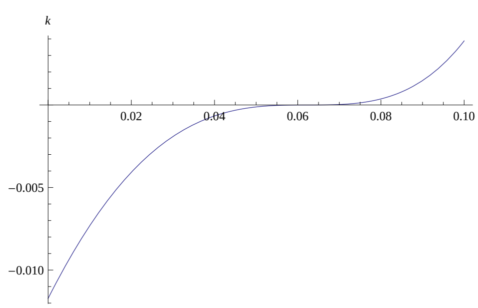


Figure 2.3: Plot of $k(4\beta + \frac{1}{4})$

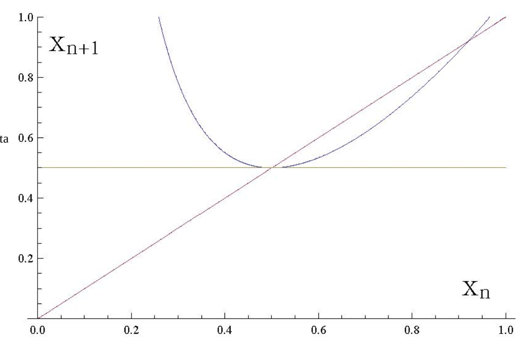


Figure 2.4: The right part of function $x_{n+1} = x_n^2 + \frac{\beta}{x_n^2}$ and the reference line $x_{n+1} = x_n$ when $\beta = \frac{1}{16}$

Therefore, when $\beta > \frac{1}{16}$, $4\beta + \frac{1}{4}$ is above the reference line. However, above the reference line does not guarantee the escape of the critical point. Actually, in this case, the critical points are on the left side of the reference line. This will force the critical points to stay bounded (when $\frac{27}{256} > \beta > \frac{1}{16}$) or escape directly (when $\beta > \frac{27}{256}$, all points on the real axis escape). As for the case $0 < \beta < \frac{1}{16}$, the critical points also stay bounded due to $k < 0$. Therefore, for all $0 < \beta < \frac{27}{256}$, the critical point does not escape. This is why $n = 2$ is a special case that there is no McMullen domain.

# Chapter 3

# Dynamics in the Plane

This chapter discusses the more broad dynamical behaviors of $f(z) = z^2 + t\frac{\beta}{z^2} + (1-t)\frac{\beta}{\overline{z}^2}$ on the complex plane. It turns out that the complex case yields much richer transition phenomena. We will talk about two main examples: a connected case and a disconnected case. But before doing that, we will discuss the critical set and the fixed points first.

## 3.1 Critical Set

The critical set is important because it can determine many fundamental structures of the dynamic plane as well as the parameter plane. For a map of the real plane, the critical set is defined by the set whose determinant of the corresponding Jacobian matrix is equal to zero. If we rewrite (1.1) to separate its real part and imaginary part

$$f(x+iy) = r(x,y) + i(x,y)I$$

The critical set is all the points that can make

$$det(J) = \begin{vmatrix} \frac{\partial r(x,y)}{\partial x} & \frac{\partial r(x,y)}{\partial y} \\ \frac{\partial i(x,y)}{\partial x} & \frac{\partial i(x,y)}{\partial y} \end{vmatrix} = 0$$

However, we will use "$z - \overline{z}$ coordinates" where $z = x + iy$. It is much easier to compute. The Jacobian matrix is

$$J = \begin{bmatrix} \frac{\partial f}{\partial z} & \frac{\partial f}{\partial \overline{z}} \\ \frac{\partial \overline{f}}{\partial z} & \frac{\partial \overline{f}}{\partial \overline{z}} \end{bmatrix} = \begin{bmatrix} 2z - 2t\beta z^{-3} & -2(1-t)\beta\overline{z}^{-3} \\ -2(1-t)\beta z^{-3} & 2\overline{z} - 2t\beta\overline{z}^{-3} \end{bmatrix} \tag{3.1}$$

Therefore let the determinant of (3.1) equal to zero and we get

$$det(J) = \frac{4}{|z|^6}(|z|^8 - t\beta z^4 - t\beta\overline{z}^4 - \beta^2 + 2t\beta^2) = 0$$

Use $x - y$ coordinates to substitute $z - \overline{z}$ coordinates. We get the critical curve

$$(x^2 + y^2)^4 + 2t\beta(x^4 - 6x^2y^2 + y^4) - \beta^2 + 2t\beta^2 = 0 \tag{3.2}$$

Use polar coordinates to simplify (3.2):

$$r^8 - 2t\beta r^4 cos4\theta - \beta^2 + 2t\beta^2 = 0 \tag{3.3}$$

or

$$r^4 = \beta(tcos4\theta \pm \sqrt{t^2cos^24\theta - 2t + 1}) \tag{3.4}$$

Equation (3.4) has an even nicer form for $\beta$ complex as well. The Jacobian matrix becomes

$$J = \begin{bmatrix} 2z - 2t\beta z^{-3} & \overline{-2(1-t)\beta z^{-3}} \\ -2(1-t)\beta z^{-3} & \overline{2z - 2t\beta z^{-3}} \end{bmatrix} \tag{3.5}$$

Therefore the determinant is

$$det(J) = (|2z - 2t\beta z^{-3}|)^2 - (|2(1-t)\beta z^{-3}|)^2$$

By letting this determinent equal to zero, we can get

$$|2z - 2t\beta z^{-3}| = |2(1-t)\beta z^{-3}|$$

In further, it can be simplified by multiplying $\frac{|z^3|}{2}$ on both sides.

$$|z^4 - t\beta| = |(1-t)\beta| \tag{3.6}$$

This nice form suggests that the fourth power of the critical point set $C^4(f)$ is actually a circle with a radius $|(1-t)\beta|$ and centered at $t\beta$.

The transition of critical set and its image from nonanalytic to analytic case is shown in Fig. 3.1

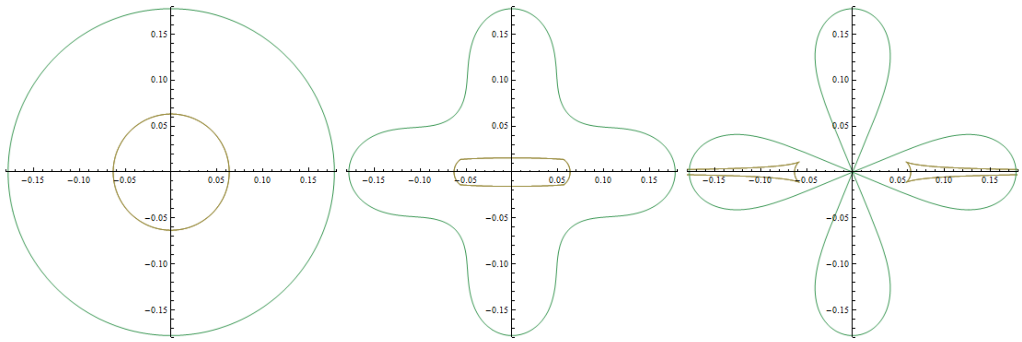

(a) $t = 0$ (b) $t = 0.47$ (c) $t = 0.5$

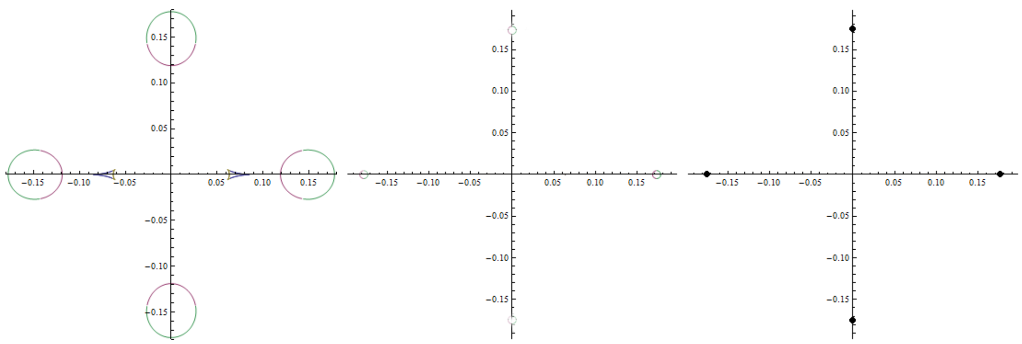

(d) $t = 0.6$ (e) $t = 0.9$ (f) $t = 1$

Figure 3.1: Transition of $C(f)$ and $V(f)$ when $\beta = 0.001$. For figure (a)-(c) the outer green curve is the $C(f)$ and the inner sienna curve is the $V(f)$. For figure (d)-(f), the four outer "circles" are the $C(f)$ and the two inner "triangles" are the $V(f)$. Note in figure (f), the four components of $C(f)$ shrink into four points and $V(f)$ in figure (e) and (f) are too small to be visible (they are close to $\pm 0.06$).

### 3.1.1 Transition of the Critical Point Set $J_0$

Since the critical set often plays an important role in the dynamical system, it is reasonable to find out the transition of the critical set before exploring the transition of the behavior of the full map. It turns out that the critical set experiences a topological change when $t = 0.5$ ($t$ goes from 0 to 1). This value does not depend on the parameter $\beta$. It turns out that there are two topological changes during this procedure. The first is the generation of the four cusps which happens at $t = 2\sqrt{3} - 3$. The second is the separation of the critical images. This happens when $t = 0.5$.

From equation (3.3), the expression of the critical set is given in polar coordinate

$$r^8 - 2t\beta r^4 cos4\theta - \beta^2 + 2t\beta^2 = 0 \tag{3.7}$$

where $\theta$ is the angle and $r$ is the radius.

Since (3.7) is in implicit form, we can solve for $r^4$ to change it into an explicit form

$$r^4 = \beta(tcos4\theta \pm \sqrt{t^2cos^24\theta - 2t + 1}) \tag{3.8}$$

By observing Fig. 3.1, it is obvious that there is a topological change which separates the single topological "circle" into four topological "circles". This transition happens when $t = 0.5$. Here is the computation. Based on the observation, when the single circle shrinks and merges into a flower with four petals, the equation

$$\theta = 0 \tag{3.9}$$

generates another solution in the origin. So let $\theta = 0$ and solve for $r$

$$\begin{aligned} r^8 - 2t\beta r^4 - \beta^2 + 2t\beta^2 = 0 \\ r^4 = \beta(t \pm \sqrt{(}t^2 - 2t + 1)) \\ = \beta(t \pm (1 - t)) \end{aligned}$$

So one solution is always $\beta$, another solution is $(2t-1)\beta$. Since $r^4$ is non negative, the second solution exists only when $t \geq 0.5$. This corresponds the moment when the four petals meet in the origin and generate the new root.

### 3.1.2 Transition of the Critical Value Set $J_1$

By using polar coordinates, the iteration map can be written as

$$Re(z_{n+1}) = \frac{\beta + r_n^4}{r_n^2} cos2\theta_n \tag{3.10}$$

$$Im(z_{n+1}) = \frac{\beta + r_n^4 - 2\beta t}{r_n^2} sin2\theta_n \tag{3.11}$$

So substituting (3.8) into this function can get the image of the critical set. The transition of the critical image set $J_1$ is shown in fig 3.2.

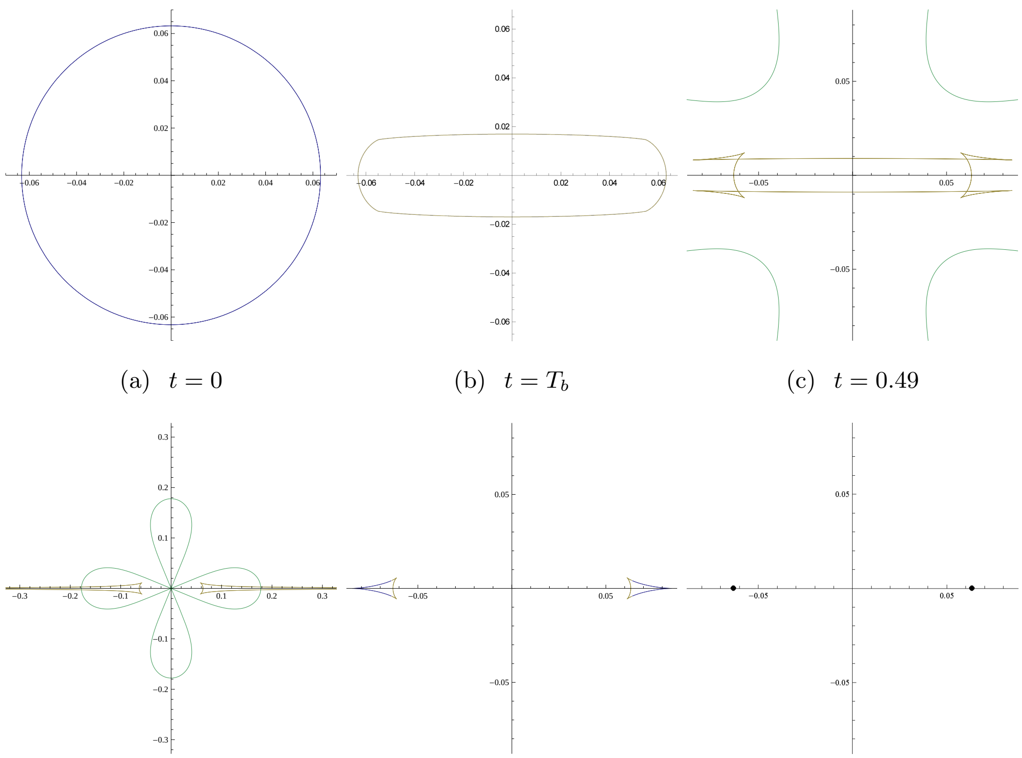

(a) $t = 0$ (b) $t = T_b$ (c) $t = 0.49$

(d) $t = 0.5$ (e) $t = 0.8$ (f) $t = 1$

Figure 3.2: Transition of $J_1$. Note that the green curves in figure (c) and (d) are the $J_0$

From the figure, we can observe two topological changes of $J_1$

1. As $t$ goes from 0 to some bifurcation point $T_b$, the $J_1$ shrinks from a circle to a curve with four swallow tails. During this period, $J_1$ is still a simple closed curve.

2. From $T_b$ to 0.5, the four tips grow into eight cusps. During this time, $J_1$ is no longer a simply closed curve but a curve with four swallow tails. These four swallow tails grow bigger and bigger. Finally, when $t = 0.5$, the two mid lines merge and disappear. The closed curve separates into two parts which look like triangles.

3. After $t = 0.5$, the two triangles become smaller and smaller and become two points at $t = 1$. These two points are exactly the two critical values for the analytic map at $t = 1$.

Here is the computation of $T_b$. Since the necessary condition for a cusp is that the tangent vector does not exist at this point. This is also equivalent to the tangent vector being $(0,0)$. So we can just let

$$D(J_1) = \overrightarrow{0}$$

where $D()$ is the derivative operator. In our case, either component of the tangent vector being equal to 0 is enough for computing the cusp points. And restrict $\theta$ between 0 and $\frac{\pi}{4}$ to avoid the symmetric solutions. We then solve for points on $J_1$ where

$$D(Re(J_1)) = 0 \tag{3.12}$$

$$0 \leq \theta \leq \frac{\pi}{4}$$

Notice that equation (3.12) should have at least one solution due to the point on the real axis. So if this equation has just one solution, then there is no cusp; if there are three solutions, then there are two possible cusps. The bifurcation value $T_b$ corresponds the case that equation (3.12) has exactly two solutions.

The real part of $J_1$ can be obtained by substituting (3.7) into (3.10). (3.7) can be written as

$$cos4\theta = \frac{r^8 - \beta^2 + 2t\beta^2}{2t\beta r^4}$$

Using the identity $2cos^2 2\theta - 1 = cos4\theta$, the real part of $J_1$ can be written as

$$Re(J_1) = \frac{\beta + r^4}{r^2}\sqrt{\frac{cos4\theta + 1}{2}}$$

Then combine these two equations and regard $r^2$ as the parameter

$$\frac{dRe(J_1)}{dr^2} = 0$$

$$\Rightarrow R^6 + t\beta R^4 - t\beta^2 R^2 + (1-2t)\beta^3 = 0 \tag{3.13}$$

in which $R = r^2$. (3.13) is a cubic equation in $R^2 = r^4$. So based on the cubic equation formula, (3.13) has three real roots among which there is a multiple root if and only if the discriminant

$$\Delta = B^2 - 4AC = 0$$

in which

$$A = t\beta - 3t\beta^2$$

$$B = t^2\beta^3 - 9(1-2t)\beta^3$$

$$C = t^2\beta^4 - 3t(1-2t)\beta^4$$

After simplification, the discriminant becomes

$$\Delta = -27\beta^6(t-1)^2(t^2+6t-3) = 0$$

The only solution when $0 < t < 0.5$ is $T_b = 2\sqrt{3} - 3$. It can be verified $D(Im(J_1)) = 0$ at these points as well. These four points turn out to be swallow tail points each which evolves into swallow tails with two nondegenerate cusps (refer to fig 3.2(c)). Note that $T_b$ does not depend on $\beta$.

## 3.2 Fixed Points

Among all the properties of a dynamical system, the distribution of the fixed points probably is the first and the easiest one that people can find out. In this section, we will try to find out the analytic expression of the fixed points. It turns out that there is no such expression. However, we still got a relatively nice equation about the fixed points which will be used in section 3.6.2.

To compute the fixed point, we prefer $x-y$ coordinates instead of polar coordinates. Therefore, $f(z)$ can be expressed as

$$f(x,y) = f_1(x,y) + f_2(x,y)i \tag{3.14}$$

where

$$f_1(x,y) = x^2 - y^2 + \frac{\beta(x^2-y^2)}{(x^2+y^2)^2}, \quad f_2(x,y) = 2xy - \frac{2\beta xy(2t-1)}{(x^2+y^2)^2} \tag{3.15}$$

Thus, letting the real part be equal to $x$ and the imaginary part be equal to $y$ gives us the equations of the fixed points. Note that in the imaginary equation, if $y \neq 0$, $y$ can be cancelled (otherwise it will reduce into the real case we have discussed in chapter 2).

$$f_1(x, y) = x^2 - y^2 + \frac{\beta(x^2 - y^2)}{(x^2 + y^2)^2} = x \tag{3.16}$$

$$f_2(x, y) = 2xy - \frac{2\beta xy(2t - 1)}{(x^2 + y^2)^2} = y \tag{3.17}$$

To handle this equation, we would like to isolate the term $(x^2 + y^2)^2$ from the second equation and subsititute into the first one. This will give us

$$\frac{x}{x^2 - y^2} = \frac{4xt - 1}{2x(2t - 1)}$$

Keep isolating $y^2$ and substitute back into the imaginary equation. This will give us a 6th degree univariate polynomial equation in $x$.

$$\beta(2t - 1)(4tx - 1)^2 = 8t^2x^3(2x - 1)^3 \tag{3.18}$$

Apparently, there is no analytic solution for this equation. But this nice form can be used to analyze the special fixed point. For instance, when $t = 0.5$, there are only two roots for $x$: 0 and 0.5. And their multiplicity are both 3. When $x = 0$, equation (3.17) forces $y = 0$ too. But $(0, 0)$ is not a fixed point. Therefore, $x = 0$ is actually not a valid root.

## 3.3 Two Different Transitions

### 3.3.1 A Connected Case: $\beta = 0.001$

Our goal is to understand the long term behaviors of dynamical system (1.1). First we would like to observe the points that have bounded orbits versus unbounded orbits. We used Matlab and Fraqtive to do this experiment. Fig. 3.3 are some graphs to show the transition of bounded orbits as $t$ varies and $\beta$ is fixed at $\beta = 0.001$. Black are bounded orbits and other colors are unbounded orbits. Note that if $\beta = 0$, the bounded orbits are exactly the unit disk.

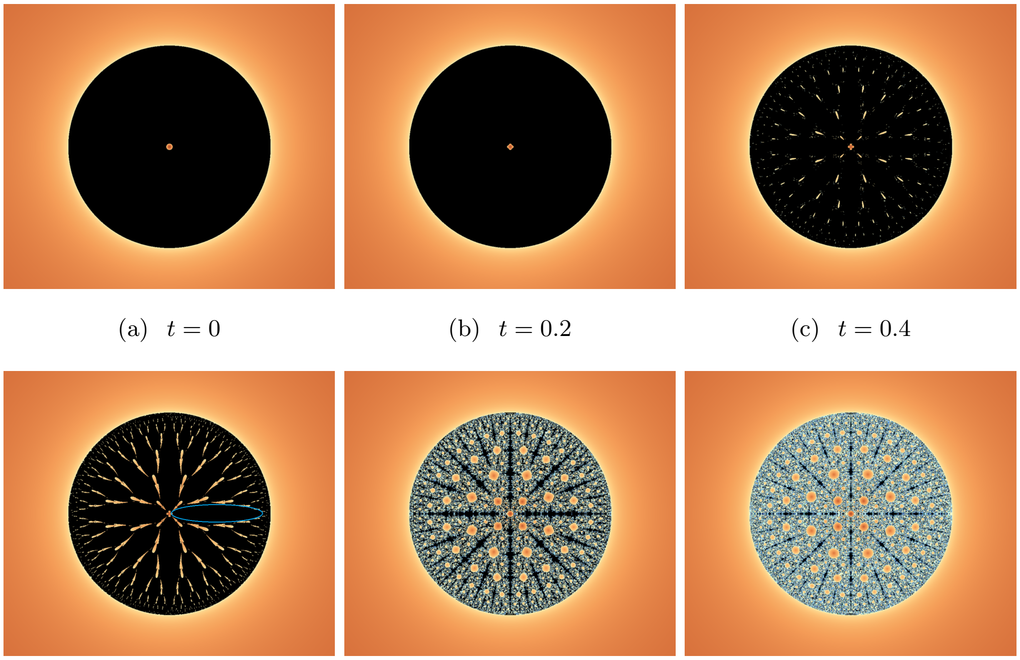

(a) $t = 0$ (b) $t = 0.2$ (c) $t = 0.4$

(d) $t = 0.5$ (e) $t = 0.9$ (f) $t = 1$

Figure 3.3: Transition of the basin of attraction with $\beta = 0.001$ and $t$ varying. All filled Julia sets appear to be connected. (a) and (f) are known to have connected filled Julia sets.

We can observe several structures in these figures.

1. The outside "circle". This is a topological circle, not a geometric circle if $t \neq 0$. Every point started outside this circle will escape to infinity.

2. There is one hole in the center. This is the so-called trap door. Every point in this trap door will map to one point outside the outside circle. Thus the trap door can be regarded as the "other" preimage of the escape region outside the outside circle.

3. The boundary of the trap door is a geometric circle at $t = 0$. It is a topological circle for $0 < t \leq 1$, but with four petals.

4. The orange dots inside the "circle" in (c)-(f) are preimages of the trap door. The

outer circle of dots has twice as many as the consecutive inner circle of dots. This is because when $|z|$ is big (far away from the origin), the $z^2$ term dominates. So the iteration map basically is similar to $z^2$, which double angles and decreases radii inside the unit circle.

5. If we define "leaf" like in Fig. 3.3(d). Then all points in "leaves" will go to the "first leaf" (indicated by blue ellipse) following a quasi angle-doubling pattern.

6. The interior of the "first leaf" is attracted to a period eight cycle on the real axis.

7. Combining the last two observations, all the interior points in the filled Julia set $K(f)$ appear to be attracted to this period eight cycle.

### 3.3.2 A Disconnected Case

This case mainly refers to the condition the positive real axis (denoted $Ray(R^+)$) escaping. Under this condition, there are many different cases which turns out much more complicated than the connected case. Six of these cases are shown in fig 3.4.

From these figures, we can find out several interesting structures

1. All the $\frac{k\pi}{4}$ rays escape. This is because all these rays will eventually map onto $Ray(R^+)$. Note that this is true even for case 2 although it is not clear from the figure.

2. There exists an escaping circle when $t$ is greater than 0.5. This circle maps onto the real axis and therefore escapes. We will explain this in following sections.

3. When $t$ is close to 0, all orbits escape. This is different from the analytic case which leaves a Cantor set bounded.

4. Cases (d) (e) and (f) have infinitely many components (we will prove this in section 3.6.) and it appears to be true for (b) and (c).

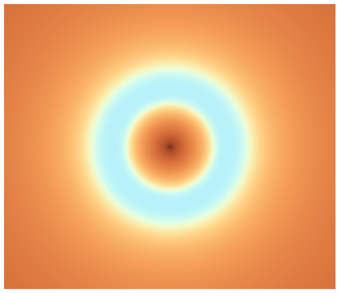
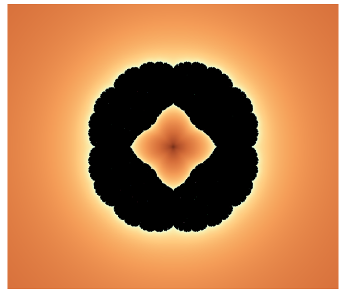
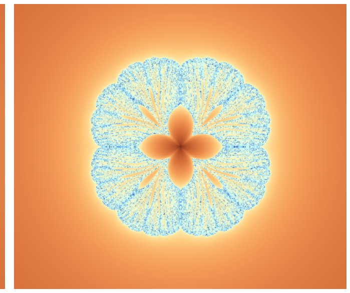

(a) Case 1: All escape ($t = 0$)

(b) Case 2: Rays escape($t = 0.2$)

(c) Case 3: Unidentified case 1($t = 0.4$)

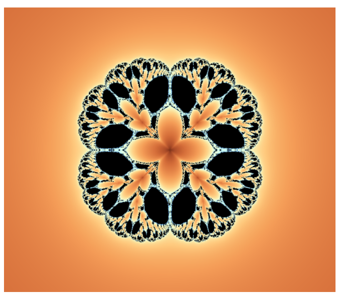
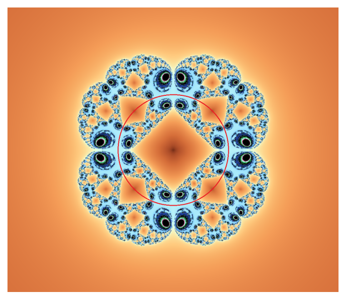
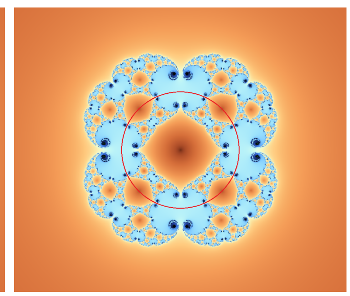

(d) Case 4: Unidentified case 2($t = 0.6$ and not all $J_0$ escapes)

(e) Case 5: Infinitely many attracting blobs($t = 0.9$ and all $J_0$ escapes)

(f) Case 6: Cantor set($t = 1$)

Figure 3.4: Transition of the basin of attraction with $\beta = 0.11$ and $t$ varying. All nonempty filled Julia sets appear to be disconnected

## 3.4 The Transition of the Parameter Plane

People are also interested in the structures of the parameter space. Here is a series of pictures of the parameter plane when $t$ varies from 0 to 1.

Note that in this picture, the parameter plane is the whole complex plane. This is different from the basic setting in this paper in which $\beta$ is a positive real number. We did this way because it can show us why the two representative cases from section 3.3 are special under a more broad background. These two cases are labeled by blue dots in fig 3.5. We will talk about them more in the following sections.

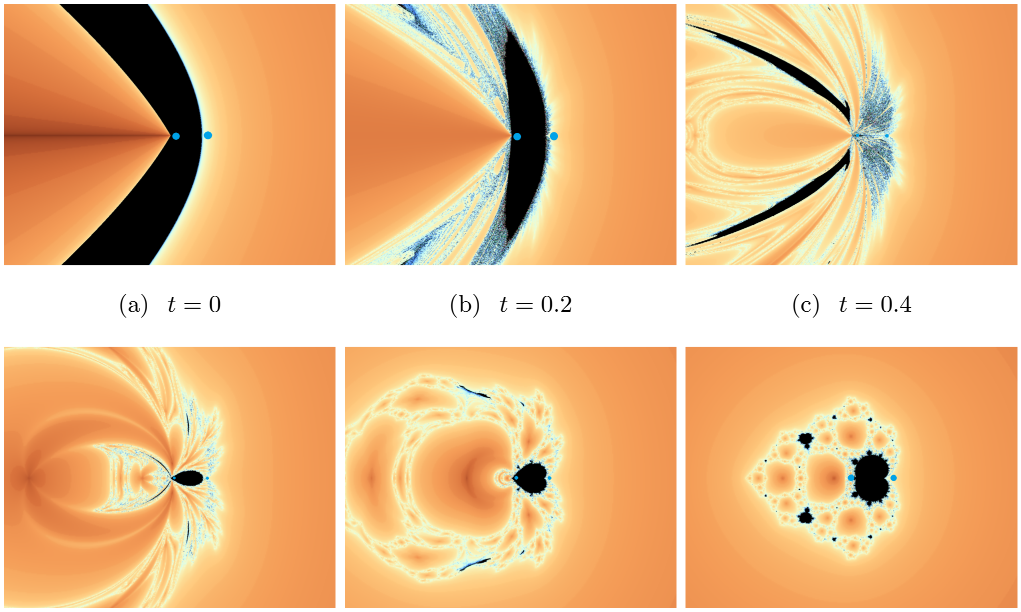

(a) $t = 0$ (b) $t = 0.2$ (c) $t = 0.4$

(d) $t = 0.6$ (e) $t = 0.8$ (f) $t = 1$

Figure 3.5: Transition of the parameter plane $\beta$ from non analytic to analytic. The $\beta$ values on the two blue dots are 0.001 and 0.11 respectively. Case (a) appears in Bozyk & Peckham's work[14] and case (f) appears in Devaney's work[6]

## 3.5 The First Transition of a Connnected $K(f)$

In the $\beta = 0.001$ case, as $t$ transits from 0.2 to 0.4, the Julia set changes from a disk with just one circular trap door to a graph consisting of numerous "white blobs". These dots are believed to be the preimages of the trap door. However, we observed that these dots do not appear one by one as $t$ goes from 0 to 1, instead, they all appear at once at a specific $t$ value. So we want to find out this $t$ as a bifurcation point.

It is easy to verify the white dots in fig 3.6 (b) are preimages of the trap door ($T_t(f)$). Since no point can map inside the critical value circle in one iteration in forward time, if there is no intersection between $T_t(f)$ and $V_t(f)$, there should be no preimage of the trap door. So computing the $t$ value of their first appearances is to compute the intersection between the boundary of the trap door and the critical value set $V_t(f)$ (image of the critical set $C_t(f)$). Fig. 3.7 illustrates the settings of this problem: the far curve from the trap door is the critical set $P_t$, the closer curve is the critical value set $V_t$, the white flower in the center is the trap door $T_t$.

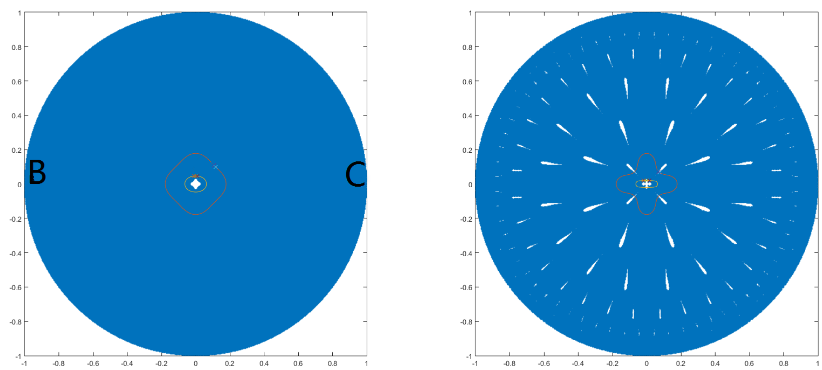


(a) Before the bifurcation, there is just one white dot in the center (t=0.2)

(b) After the bifurcation, there appears numerous white dots immediately (t=0.4)

Figure 3.6: Trap door and its preimages for $\beta = 0.001$

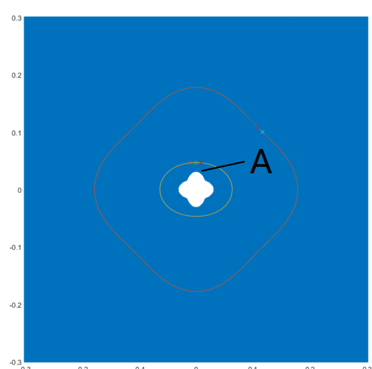


Figure 3.7: Zoom-in view of figure 3.6(a): Trap door is totally inside the critical value set $V(f)$

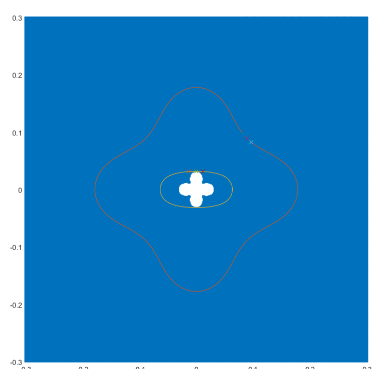

Figure 3.8: $V(f)$ is tangent to the boundary of the trap door $T(f)$ when $t = 0.374749$ ($\beta = 0.001$)

From this figure, we can easily find out that the intersection point is the tangent point of the $T_t$ and $V_t$. So we just need to compute the value of the tip A and the maximum point of $V_t$ (by symmetric properties of $f(z)$, see section 3.6.1). $A = (0, x_2)$ is one of the preimages of $B = (-x_1, 0)$ and $C = (x_1, 0)$ is the fixed point. So the image value of point $B$ is determined by

$$\begin{cases} x_1 = x_1^2 + \frac{\beta}{x_1^2} \\ -x_1 = x_2^2 + \frac{\beta}{x_2^2} \end{cases} \tag{3.19}$$

Note in this equation set, we use the real part to compute the imaginary part of point A. This is true because $f(A) = B$, $f(B) = C$ and $f(C) = C$.

To solve equation (3.19), we can get the position of point A. So next step will be find the top point of the $V_t$. This can be done by calculating the derivative of the imaginary part of the $V_t$ curve. The imaginary part of any $f(z_{r,\theta})$ is

$$image = \frac{\beta + r^4 - 2\beta t}{r^2} sin2\theta \tag{3.20}$$

The equation for the critical curve is

$$r^4 = \beta(tcos4\theta \pm \sqrt{t^2cos^2 4\theta - 2t + 1}) \tag{3.21}$$

or

$$cos4\theta = \frac{r^8 - \beta^2 + 2t\beta^2}{2t\beta r^4} \tag{3.22}$$

Plug equation(3.22) into equation(3.20) by the identity

$$sin^2 2\theta + cos^2 2\theta = 1$$

We can get the expression of the imaginary part of the critical value set $V_t$. Then compute the derivative with respect to $r^2$

$$\frac{d(image)}{dr^2} = 0 \tag{3.23}$$

By using Mathematica, the solution of equation(3.23) is

$$r^2 = \sqrt{\frac{\beta - \beta t \pm \beta\sqrt{t^2 + 6t - 3}}{2}} \tag{3.24}$$

Then plug this solution back into equation(3.20) to get the maximum of $V_t$, denoted $p_{vt}$. Let this maximum equal to the value of $x_2$ from equation(3.19).

$$p_{vt} = x_2$$

The solution of this equation is the bifurcation point of t. Since the symbolic expression with respect to $\beta$ is very complicated, we just compute one numerical example for $\beta = 0.001$. The $t$ value for the first bifurcation is $t = 0.374749$ (as shown in fig 3.8).

## 3.6 The Transition of a Disconnnected $K(f)$

### 3.6.1 The Investigation Tools

Before we talk about the structures of $K(f)$, we would like to introduce the tools we used in our investigation. These tools are just some topological properties from the map itself therefore do not rely on the complex analytic condition.

1. *Symmetric properties of $f(z)$*
   It is easy to verify these facts: 1) rotate 180: $f(z) = f(-z)$; 2) rotate 90: $f(iz) = -f(z)$; 3) from 1 and 2: $f^2(iz) = f^2(z)$; 4) conjugate respect to x and y axes: $f(\overline{z}) = \overline{f(z)}$, $f(-\overline{z}) = \overline{f(z)}$; 5) combining properties above, the $J(f)$ and $K(f)$ are symmetric with repect to the x axis, y axis and $\theta = \frac{\pi}{4} + \frac{k\pi}{2}$ lines.

2. *The dynamical behaviors on the real and imaginary axes are not affected by t*
   This is true because if we restrict $f(z)$ on real, the map will become

   $$f(x) = x^2 + \frac{\beta}{x^2}$$

   which is determined only by $\beta$. In further, because of $f(z) = f(-z)$, the dynamical behaviors on $R^-$ is the same as on $R^+$. This is to say, if $R^+$ escapes, $R^-$ also escapes. If $R^+$ has an invariant region, then $R^-$ also has a symmetric bounded region (Note this region is not invariant because $f(z) = f(-z)$). We denote the points on $R^+$ as $Ray(R^+)$ and the points on $R^-$ as $Ray(R^-)$. So $f(Ray(R^-)) = Ray(R^+)$.

   For the points on the imaginary axis, after one iteration, they will map to the real axis. Therefore, the bounded region on the imaginary axis is a $90^o$ rotation of the bounded region on the real axis. We denote the points on $I^+$ as $Ray(I^+)$ and the points on $I^-$ as $Ray(I^-)$. Thus

$$f^2(Ray(I^+)) = f(Ray(R^-)) = Ray(R^+)$$

$$f^2(Ray(I^-)) = f(Ray(R^-)) = Ray(R^+)$$

3. *The points with an angle of $\frac{\pi}{4} + \frac{k\pi}{2}$ are mapped onto the imaginary axis*
   This property is pretty straight forward if we write $f(z)$ into polar coordinate

$$Re(z_{n+1}) = \frac{\beta + r_n^4}{r_n^2} cos2\theta_n \tag{3.25}$$

$$Im(z_{n+1}) = \frac{\beta + r_n^4 - 2\beta t}{r_n^2} sin2\theta_n \tag{3.26}$$

   So from the real part equation, if $\theta_n = \frac{\pi}{4} + \frac{k\pi}{2}$, then $Re(z_{n+1})$ is always equal to 0. This property shows that the rays with angles $\frac{\pi}{4}$, $\frac{3\pi}{4}$, $\frac{5\pi}{4}$, $\frac{7\pi}{4}$ are four preimages of the imaginary axis. We denote these four rays as $Ray(\frac{\pi}{4})$, $Ray(\frac{3\pi}{4})$, $Ray(\frac{5\pi}{4})$, $Ray(\frac{7\pi}{4})$. These rays can be called prepole rays because they go through the four prepoles when $t > 0.5$.

4. *When $t > 0.5$, the circle $r = \sqrt[4]{\beta(2t-1)}$ is mapped onto the real axis*
   It is easy to check $Im(z_{n+1}) = 0$ if we plug $r = \sqrt[4]{\beta(2t-1)}$ into the iteration formula (3.26). This shows that the image of the circle is a line segment of the real axis. Notice that $(\sqrt[4]{\beta(2t-1)}, 0)$ is also a point of the the critical set. So we denote this circle as critical circle $Cir_c$

5. *Combine 3 and 4, we have: 1) when $t > 0.5$, $Cir_c$ and the four prepole rays have four intersections. These four intersections are the four prepoles. 2) when $t \leq 0.5$, there is no prepole and the critical set merges into one closed curve*

We will use these tools intensively in the following investigations. You will find that the interaction of these rays and the critical set plays an important role in the construction of $K(f)$. Fig. 3.9 shows the geometry of these tools.

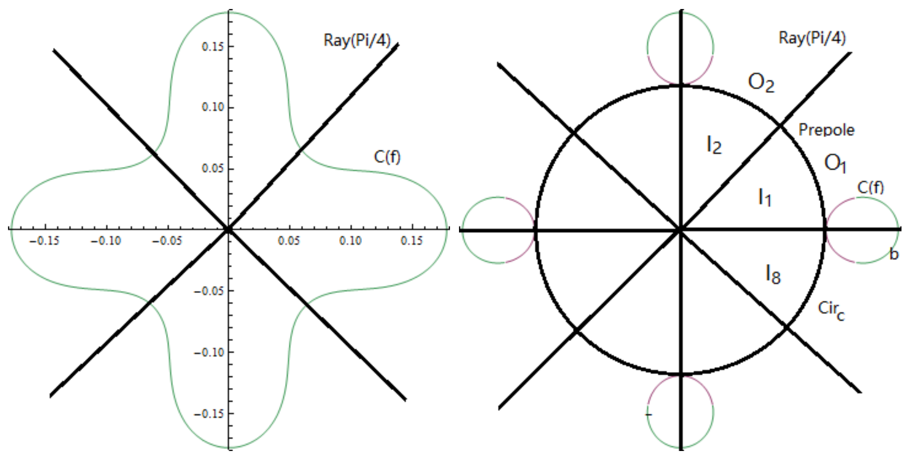


(a) $t < 0.5$

(b) $t > 0.5$

Figure 3.9: Rays and the critical point set $C(f)$

### 3.6.2 Structure of $J(f)$

In this section, we will discuss some basic structures of the filled Julia set when the real axis escapes. As shown in fig 3.4, this includes several different cases

**Proposition.** *When $t > 0.5$ and $Ray(R^+)$ ($\beta > \frac{27}{256}$) escapes, $K(f)$ has infinitely many components*

Proof: To prove this proposition, we would like to implement the similar idea as in the proof that $J(f)$ is a Cantor set for $z^2 + c$ when the critical orbit escapes. That is, trying to prove the statement by constructing the $K(f)$. The only difference in this proof is that we will use the preimages of $Ray(R^+)$ and the symmetric properties of the map itself to construct the "escaping spines" that can isolate the components of $K(f)$. Here is the construction procedure.

Step 1: Construct the immediate escaping spines.

Based on our analysis in section 3.6.1, when $t > 0.5$, the basic setting of rays and critical set are shown in fig 3.10. $Z_1$, $Z_2$, $Z_3$ and $Z_4$ are the four prepoles. The circle going through these four prepoles and centered at origin is the so-called critical circle. The four small elipse-like curves outside the critical circle are the four components of the critical set $C(f)$. From the computation in section 3.6.1, $C_v = \sqrt[4]{\beta(2t-1)}$

and $C_f = \sqrt[4]{\beta}$. So when $t$ varies, $C_f$ will stay fixed while $C_v$ moves along the $R^+$ axis. Also from above section, all the rays and the critical circle will eventually map on $Ray(R^+)$. Therefore, if $Ray(R^+)$ escapes, then all these rays and circles will also escape; if $Ray(R^+)$ stays bounded, then all these rays and circles will stay bounded. Since $Ray(R^+)$ escapes in our case, all the prepole rays, the axis rays and the critical circle also escape. This sketches the first structure of the "escaping spines".

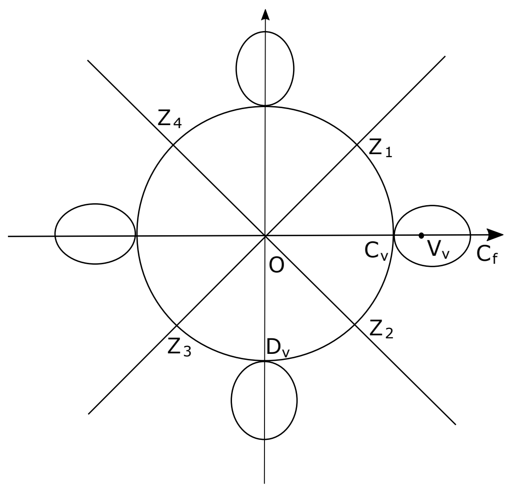


Figure 3.10: The critical set and rays when $t > 0.5$

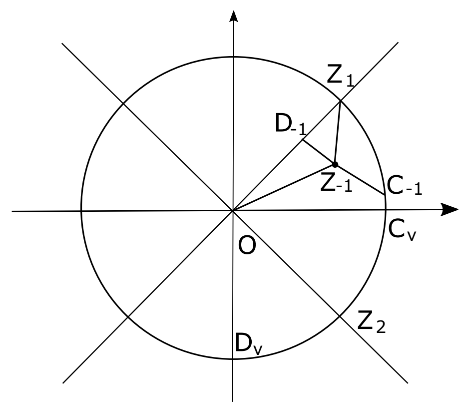


Figure 3.11: Step 2: preimages of the escaping spine

As shown in fig 3.10, these "escaping spines" divide the complex plane into sixteen separate regions. Since all these spines escape, the components of $K(f)$ can only appear inside each region. For simplicity, in following steps, we will just focus on the interior of sector $OC_vZ_1$. If we can prove the proposition on this sector, then the conclusion on the entire complex plane will be automatically guaranteed by the symmetry properties.

Step 2: Construct the escaping spines inside the sector $OC_vZ_1$ by finding the preimages of the immediate escaping spines. Apparently, the preimages of the escaping spines should also escape.

However, we still don't know where to find these preimages. To do this, we should first know the mapping property of sector $OC_vZ_1$ under the iteration formula $f(z)$. This can be done by both numerical experiment and analytic deduction. It turns out that the sector $OC_vZ_1$ will be mapped onto the entire fourth quadrant of the complex plane. To make it precise, here are some statements about the map $f(z)$ restricted on sector $OC_vZ_1$.

1. *$f(z)$ maps the interior of sector $OC_vZ_1$ one to one and onto the fourth quadrant of the complex plane*

   To verify this statement, just consider the equation (3.25) and equation (3.26). When $0 < \theta_n < \frac{\pi}{4}$, both $cos2\theta_n$ and $sin2\theta_n$ are positive. When $r < \sqrt[4]{\beta(2t-1)}$ (inside the critical circle), $\frac{\beta+r_n^4}{r_n^2}$ is always positive but $\frac{\beta+r_n^4-2\beta t}{r_n^2}$ is negative. Therefore, after one iteration, $Re(z_{n+1})$ stay positive but $Im(z_{n+1})$ becomes negative. This corresponds the fourth quadrant.

   However, being inside is not enough to say it is "onto" the fourth quadrant. So we still need to show that the image of sector $OC_vZ_1$ actually covers the entire fourth quadrant.

   To do this, let us pick any point in the fourth quadrant, say $P = x - yi$, in which both $x$ and $y$ are positive. Then let $x$ be equal to equation (3.25) and $-y$ be equal to equation (3.26). The solution of this equation set should give us all the preimages of point $P$.

$$\begin{aligned} \frac{\beta+r^4}{r^2}cos2\theta &= x \\ \frac{\beta+r^4-2\beta t}{r^2}sin2\theta &= -y \end{aligned} \tag{3.27}$$

   By using a trigonometric identity, we can eliminate the unknown $\theta$ first. So equation (3.27) will become

$$(\frac{r^2x}{\beta+r^4})^2 + (\frac{r^2y}{\beta+r^4-2\beta t})^2 = 1 \tag{3.28}$$

   Obviously, this is a univariate rational equation in $r$. Note that the denominators of the left two fractions will never be zero due to our restriction on the interior of sector $OC_vZ_1$. Let's denote this rational map by $R(r)$

$$R(r) = (\frac{r^2x}{\beta+r^4})^2 + (\frac{r^2y}{\beta+r^4-2\beta t})^2 - 1 \tag{3.29}$$

   Then it is easy to find

$$\lim_{r\to 0^+} R(r) = -1$$

$$\lim_{r \to \sqrt[4]{\beta(2t-1)}} R(r) = \infty$$

Therefore, because rational map is always continuous on its domain, there exists at least one solution for the equation $R(r) = 0$ on the interval $(0, \sqrt[4]{\beta(2t-1)})$. After we get the solution $r$, it is easy to find a solution for $\theta$ by solving

$$cos2\theta = \frac{r^2 x}{\beta + r^4}$$

Notice that this equation always has one and only one solution between 0 and $\frac{\pi}{4}$ ($cos2\theta : (0, \frac{\pi}{4}) \to (0, 1)$ is monotonic).

Thus, combining all the analyses above, we can now say that $f(z)$ maps the interior points of sector $OC_vZ_1$ "onto" the entire fourth quadrant of the complex plane.

As for the one-to-one map, we just need to show that equation (3.28) has only one solution in sector $OC_vZ_1$. This can be done by analyzing the monotonic property of $R(r)$. A good way to do this is to write $R(r)$ as

$$R(r) = \frac{x^2}{(\frac{\beta}{r^2} + r^2)^2} + \frac{y^2}{(\frac{(2t-1)\beta}{r^2} - r^2)^2} - 1 \tag{3.30}$$

Then the problem is transformed into an easier one: analyzing the monotonic property of the two denominators. It is easy to verify that both of the denominators are decreasing on the interval $(0, \sqrt[4]{\beta(2t-1)})$ (Note that $\sqrt[4]{\beta(2t-1)} < \sqrt[4]{\beta}$). Therefore, $R(r)$ is increasing on the interval $(0, \sqrt[4]{\beta(2t-1)})$. Combining our previous conclusion, we can get immediately that $R(r) = 0$ has exactly one solution. This completes the "one-to-one" part of this statement.

2. *$f(z)$ maps the boundary of sector $OC_vZ_1$ onto the $R^+$ and $I^-$ axes. Specifically, $f(z)$ maps arc $Z_1C_v$ onto line segment $OV_v$, line segment $OC_v$ onto the positive real axis starting at point $V_v$ (the image of $C_v$) and maps $OZ_1$ onto ray $Ray(I^-)$*

   These facts come directly from the properties in section 3.6.1.

3. *For a continuous curve $\gamma(\phi)$ inside the fourth quadrant but outside the critical set, there is exactly one preimage $f^{-1}(\gamma(\phi))$ in sector $OC_vZ_1$ and this preimage is also a continuous curve*

The uniqueness of $f^{-1}(\gamma(\phi))$ can be obtained from the statement #1 immediately. We just need show that $f^{-1}(\gamma(\phi))$ is also continuous.

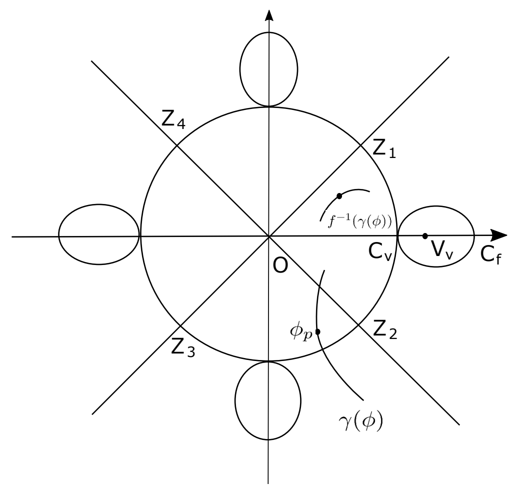


Figure 3.12: Curve $\gamma(\phi)$ and its preimage $f^{-1}(\gamma(\phi))$

Firstly, plug the curve $\gamma(\phi) = x(\phi) - y(\phi)i$ into the equation (3.28). This will give us the relationship between $r$ and $\phi$.

$$(\frac{r^2x(\phi)}{\beta + r^4})^2 + (\frac{r^2y(\phi)}{\beta + r^4 - 2\beta t})^2 = 1 \tag{3.31}$$

Then compute the right limit of $r(\phi)$ at any given point $\phi_p$

$$(\frac{(\lim_{\phi\to\phi_p^+} r(\phi))^2x(\phi_p)}{\beta + (\lim_{\phi\to\phi_p^+} r(\phi))^4})^2 + (\frac{(\lim_{\phi\to\phi_p^+} r(\phi))^2y(\phi_p)}{\beta + (\lim_{\phi\to\phi_p^+} r(\phi))^4 - 2\beta t})^2 = 1 \tag{3.32}$$

Notice that we use $x(\phi_p)$ and $y(\phi_p)$ instead of $\lim_{\phi\to\phi_p^+} x(\phi)$ and $\lim_{\phi\to\phi_p^+} y(\phi)$. This is because $x(\phi)$ and $y(\phi)$ are continuous functions, $\lim_{\phi\to\phi_p^+} x(\phi)$ is actually equal to $x(\phi_p)$ and $\lim_{\phi\to\phi_p^+} x(\phi)$ is equal to $y(\phi_p)$.

Using the same technique, we can get the similar equation of the left limit of $r(\phi)$ at $\phi_p$

$$(\frac{(\lim_{\phi\to\phi_p^-} r(\phi))^2x(\phi_p)}{\beta + (\lim_{\phi\to\phi_p^-} r(\phi))^4})^2 + (\frac{(\lim_{\phi\to\phi_p^-} r(\phi))^2y(\phi_p)}{\beta + (\lim_{\phi\to\phi_p^-} r(\phi))^4 - 2\beta t})^2 = 1 \tag{3.33}$$

These two equations have the same parameters but different unknowns. Therefore, $\lim_{\phi\to\phi_p^+} r(\phi)$ and $\lim_{\phi\to\phi_p^-} r(\phi)$ are actually two solutions of the equation $R(r) = 0$. But from the conclusion in the first statement, this equation has only one solution inside the sector $OC_vZ_1$. Therefore, the left limit has to be equal to the right limit. This completes the continuity proof. This proof is shown in fig 3.12

Note that we don't require that this curve is a Jordan curve. Our construction of the escaping spine will also work even if it is self intersecting.

After clarifying the mapping properties of $f(z)$ on sector $OC_vZ_1$, we now can construct the escaping spine inside this sector by finding the preimages of the existing spines in the fourth quadrant.

First, find the preimages of prepole $Z_2$, origin $O$ and the critical points $C_v$, $D_v$. Based on statements 1 and 2, the preimage of prepole $Z_2$ should be inside sector $OC_vZ_1$, the preimage of $O$ is $Z_1$, the preimage of $C_v$ is on the arc $C_vZ_1$, the preimage of $D_v$ is on the line segment $OZ_1$. They are denoted as $Z_{-1}$, $C_{-1}$ and $D_{-1}$, which means the first construction.

Correspondingly, the preimages of arc $D_vZ_2$, arc $C_vZ_2$, line segment $OZ_2$ and the ray starting from $Z_2$ to infinity can be obtained immediately based on statement 3. Fig 3.11 shows these preimages. Note that we didn't draw the critical set in this picture.

Step 3: Construct the escaping spines in sector $OD_vZ_2$ and $OZ_2C_v$ by symmetric properties.

Based on the $90^o$ rotational symmetry, the escaping spines in sector $OD_vZ_2$ can be obtained immediately. Based on the conjugate property with respect to the x axis, we can also get the escaping spines in sector $OZ_2C_v$. These new points are denoted by superscripts "r" and "c" to indicate that they are obtained by rotational and conjugate symmetries. This step was shown in fig 3.13.

Step 4: Repeat step 2 and step 3 to find more preimages of the current escaping spines.

This is to say, at first, using the inverse mapping properties (three statements above) to find the preimages in sector $OC_vZ_1$ which will map to the new escaping spines in the fourth quadrant. Then use the symmetric properties to generate more escaping spines in the fourth quadrant. But be careful, for each stage, we can only refine two sections of the current partition. For instance, since $Z_{-1}$ maps to $Z_2$ and $C_{-1}$ maps to $C_v$, $Z_1Z_{-1}$

will map to $OZ_2$, $Z_{-1}C_{-1}$ will map to $Z_2C_v$ and $C_{-1}Z_1$ will map to $OC_v$. This shows that the section $Z_{-1}C_{-1}Z_1$ actually maps to the whole sector $OZ_2C_v$. Therefore, the preimages of the new escaping spines in sector $OZ_2C_v$ should be only inside partition $Z_{-1}C_{-1}Z_1$. Similarly, the preimages of the escaping spines inside sector $OZ_2D_v$ should be inside section $D_{-1}Z_{-1}Z_1$. The new preimages are shown in fig 3.14.

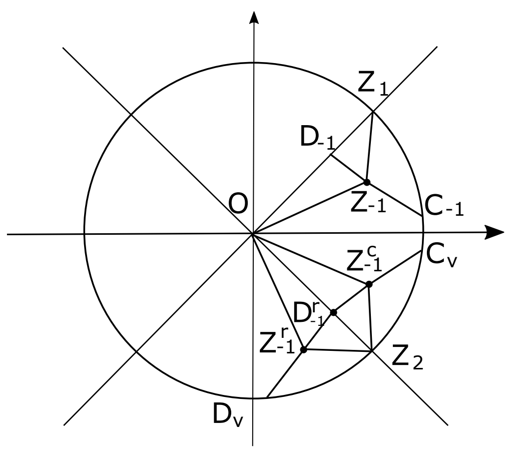


Figure 3.13: Step 3: construct the new escaping spines in the fourth quadrant by using symmetric properties

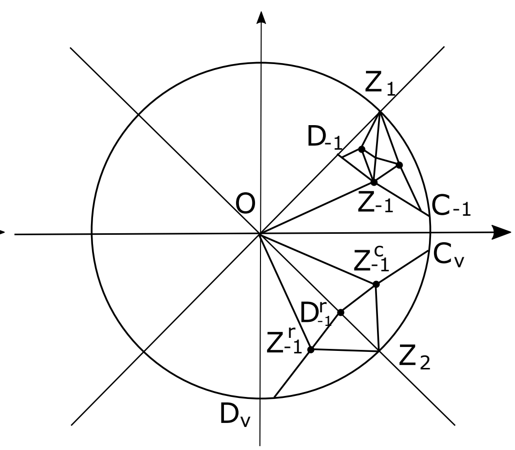


Figure 3.14: Step 4: find the more preimages in sector $OC_vZ_1$ by using mapping properties

Note that in these figures, the escaping spines are not necessarily lines. We just use it to represent curves although the $Ray(\frac{\pi}{4} + \frac{k\pi}{2})$ are indeed geometric lines (see section 3.6.1).

Therefore, keep doing this construction, we will get a partition of sector $OC_vZ_1$. And all the partition curves will eventually map onto the $Ray(R^+)$. Since $Ray(R^+)$ escapes, all these partition curves will also escape.

So far, we have constructed a partition of sector $OC_vZ_1$ which consists of many escaping spines. But we still don't know if there is a component of $J(f)$ inside each isolated section. There could be nothing inside each section. Therefore, we still need to show that there are at least infinitely many points in sector $OC_vZ_1$ that are isolated by the escaping spines. The following proof mainly refers to fig 3.15

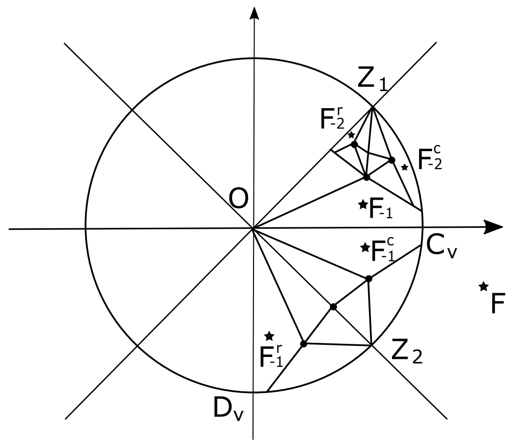


Figure 3.15: The eventually fixed points in sector $OC_vZ_1$

We will use the eventually fixed points to show these infinitely many components. So at first, pick a fixed point $F$ in the fourth quadrant (There is always a fixed point in the fourth quadrant given the conditions $0.5 < t$ and $Ray(R^+)$ escaping). For simplicity, we assume $F$ lies outside the sector $OZ_2C_v$. We will show in the following proof that the actual position of this fixed point does not matter because the image of the sector $OZ_1C_v$ covers the entire fourth quadrant.

Then find the preimages of this fixed point and their symmetric points in the fourth quadrant like in step 2 and step 3. Keep doing this procedure so that we can get infinitely many eventually fixed points. Note that any two of these eventually fixed points are distinct and disconnected with each others because they belongs to different sections which are isolated by the escaping spines.

After finding these prefixed points, a binary representation map can be established. The pattern of generating the prefixed points is shown in fig 3.16. We can label all the points whose images were generated by conjugate symmetry as “0” and all the points whose image was generated by rotational symmetry as “1”. Therefore, every prefixed point in sector $OZ_1C_v$ corresponds a binary number between 0 and 1. For instance, $F^r_{-2}$ corresponds number 0.1 and $F^{cr}_{-3}$ corresponds 0.01. This completes the “infinitely many” components of $K(f)$ proof.

$$\begin{tikzcd}
 & & & & F^{rr}_{-2} \arrow[r] & F^{rr}_{-3} \\
 & & F^{r}_{-1} \arrow[r] & F^{r}_{-2} \arrow[ur] \arrow[dr] & & \\
 & & & & F^{rc}_{-2} \arrow[r] & F^{rc}_{-3} \\
F \arrow[r, dash] & F_{-1} \arrow[uur] \arrow[ddr] & & & & \\
 & & & & F^{cr}_{-2} \arrow[r] & F^{cr}_{-3} \\
 & & F^{c}_{-1} \arrow[r] & F^{c}_{-2} \arrow[ur] \arrow[dr] & & \\
 & & & & F^{cc}_{-2} \arrow[r] & F^{cc}_{-3}
\end{tikzcd}$$

Figure 3.16: The generation pattern of the prefixed points in sector $OC_vZ_1$

Since the proposition shows us that the number of $J(f)$ components are infinitely many, we naturally want to know if these components constitute a Cantor set. This is reasonable because this set is a Cantor set [6] when $t = 1$. However, the computation shows that $J(f)$ is no longer a Cantor set for some combination of $t$ and $\beta$.

**Proposition.** *When $t > 0.5$ and $Ray(R^+)$ escapes, there exists a parameter region $NC$ such that when $(t, \beta) \in NC$, $K(f)$ is no longer a Cantor set*

Proof: If $K(f)$ is a Cantor set, it is totally disconnected. This precludes any attracting periodic orbits. Thus we just need to show that when $(t, \beta) \in NC$, the fixed points of $f(z)$ are actually attracting. This can be done by computing the determinant of the Jacobian matrix. If the determinant is less than one, then the fixed point is attracting.

This trick can work because when $Ray(R^+)$ escapes, the fixed points are two pairs of conjugate points. And the corresponding Jacobian matrix has two conjugate eigenvalues. Thus, the determinant of the Jacobian matrix is actually equal to the square of the modulus of the eigenvalues. The determinant can be computed easily by

$$Det(J) = Det(\begin{bmatrix} \frac{\partial r(x,y)}{\partial x} & \frac{\partial r(x,y)}{\partial y} \\ \frac{\partial i(x,y)}{\partial x} & \frac{\partial i(x,y)}{\partial y} \end{bmatrix}) \tag{3.34}$$

This formula refers to equation (3.14).

Then we need to evaluate $Det(J)$ at the fixed point. But from section 3.2, there is no analytic solution for the fixed points. This means there should be no way to compute $Det(J)$ directly. However we could still prove the proposition by using the Intermediate Value Theorem. Firstly, we observed that $Det(J)(t, \beta)$ is a continuous function of $t$ and $\beta$ if $x$ and $y$ are not equal to zero at the same time. Secondly, the $Det(J)$ can be found easily when $t = 0.5$. From section 3.2, one fixed point is $(0.5, y_f(\beta))$. Plug this point into formula (3.34) and we can get a function $Det(J)(0.5, \beta)$. Since this function is very complicated, a numerical approximation is used here. The computation shows that

$$Det(J)(0.5, 0.11) = 0.973 < 1$$

$$Det(J)(0.5, 0.12) = 1.149 > 1$$

Since $Det(J)(t, \beta)$ is continuous and we have already know that $Det(J) > 1$ (because $K(f)$ is a Cantor set, refer [6]) at $t = 1$, there should exists a critical combination $(T_c, \beta_c)$ such that when $\beta < \beta_c$ and $t > T_c$, the fixed points are actually attracting. Thus $K(f)$ is no longer a Cantor set. The combination $(T_c, \beta_c)$ constitutes the boundary of region $NC$.

Further investigation shows that $f(z)$ is actually semiconjugate to the full shift on 4 symbols. Since the symbolic dynamics is well known, this semiconjugacy actually provides us a way to largely understand the dynamical behaviors.

**Theorem.** *When $t > 0.5$ and Ray$(R^+)$ escapes, the map $f(z)$ is semiconjugate to the full shift on 4 symbols*

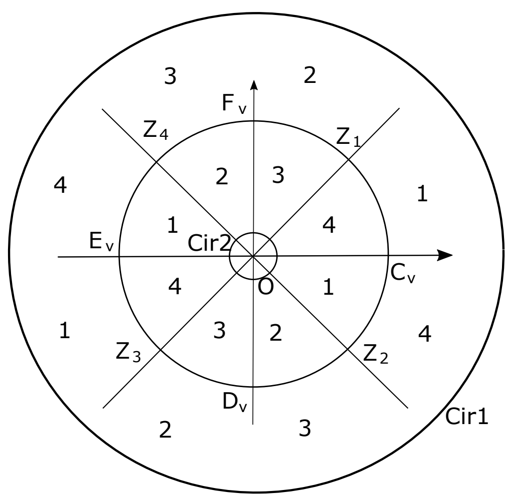


Figure 3.17: The mapping properties for each sector and region

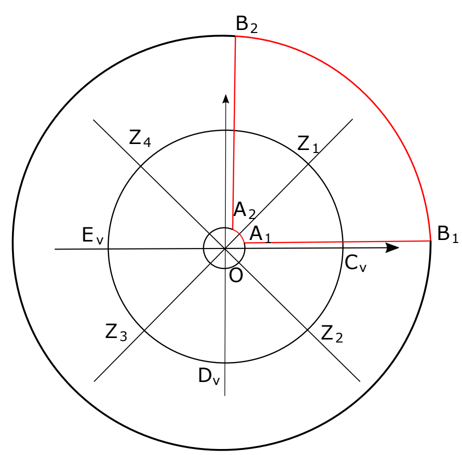


Figure 3.18: The compact set in the first quadrant

Proof: Based on the statements during the proof of the first proposition, sector $OC_vZ_1$ maps onto the fourth quadrant. Using the same technique, we can prove that the region (denoted by region $C_vZ_1$) outside sector $OC_vZ_1$ in the first $\frac{\pi}{4}$ section (bounded by $Ray(0)$ and $Ray(\frac{\pi}{4})$) also maps onto the first quadrant. The mappings for other sectors and their outside regions can be obtained immediately by the symmetric properties. These mapping properties are shown in figure 3.17. The number in each sector denotes the quadrant it will cover after one iteration. One interesting fact shown by these mappings is that the four fixed points can only appear inside region $C_vZ_1$, region $C_vZ_2$, sector $OZ_4F_v$ and sector $OZ_3D_v$ because these are the only regions whose images cover themselves.

Therefore, after one iteration, each quadrant covers the whole plane. Since $f(z) \approx z^2$ when $z$ is big, we can always find a circle $Cir1$ outside which all points escape and the preimage of this circle (denoted by $Cir2$) near the origin. And because $Ray(R^+)$ escapes, we can find one curve $A_1B_1$ near the real axis and one curve $A_2B_2$ near the imaginary axis that only the points between $A_1B_1$ and $A_2B_2$ in the first quadrant could stay. Therefore, curve $A_1B_1$, curve $A_2B_2$, arc $A_1A_2$ and arc $B_1B_2$ enclose a compact set (illustrated in figure 3.18 by red boundaries) which contains all the non escape points in the first quadrant. Using the same technique, we can construct similar regions for the rest three quadrants. Denote these four regions by four symbols $R_0$, $R_1$, $R_2$ and $R_3$. Therefore, each orbit for the non escape points in the four quadrants corresponds to a sequence in four symbols. And the iteration operation in the sequence space is a shift map:

$$\begin{array}{ccc} \Lambda & \xrightarrow{f} & \Lambda \\ S\downarrow & & S\downarrow \\ \Sigma & \xrightarrow[\sigma]{} & \Sigma \end{array} \tag{3.35}$$

where $\Lambda$ consists of non escape points and the sequence space $\Sigma$ is defined by

$$\Sigma = \{(s_0s_1s_2\ldots)|s_j = 0, 1, 2, or 3\}$$

The shift map and the itinerary map are defined as follow

$$\sigma(s_0s_1s_2\ldots) = (s_1s_2s_3\ldots)$$

$$S(z) = (s_0s_1s_2\ldots)\ where\ s_j = i\ if\ f^j(z)\ is\ in\ R_i$$

Thus, to show $f$ and $\sigma$ are semiconjugate, we need to prove (1) $f$, $S$ and $\sigma$ are continuous (2) $S \circ f(z) = \sigma \circ S(z)$ (3) $S$ is onto but not one to one.

The continuity of $f$ is trivial by the formula itself. And the continuities of $\sigma$ and $S$ are well-known (refer to [16]). The commutativity of diagram3.35 is quite straightforward. Suppose $z \in \Lambda$ has itinerary $(s_0 s_1 s_2 \dots)$, then by definition

$$S \circ f(z) = S(f(z)) = (s_1 s_2 \dots) = \sigma((s_0 s_1 s_2 \dots)) = \sigma \circ S(z)$$

$S$ is a surjection because for any sequence in $\Sigma$, say $(s_0 s_1 s_2 \dots)$, there exists a sequence of nested compact sets

$$R_{s_0} \supset R_{s_0 s_1} \supset R_{s_0 s_1 s_2} \supset \cdots \supset R_{s_0 s_1 s_2 \dots}$$

where $R_{s_0 s_1 s_2 \dots s_n} = \{z \in \Lambda | z \in R_{s_0}, f(z) \in R_{s_1}, \dots, f^n(z) \in R_{s_n}\}$. Then by the theorem of nested compact sets, $\bigcap_{n \geq 0} R_{s_0 s_1 s_2 \dots s_n}$ is nonempty. But $S$ is obviously not one to one because figure 3.4(e) shows that all the points in one blob have the same itinerary.

This completes the semiconjugacy of $f$ and $\sigma$. For $t = 1$ (analytic case), it is known to be a conjugacy[6].

**Corollary.** *When $t > 0.5$ and Ray$(R^+)$ escapes, $K(f)$ actually has uncountable infinitely components*

Proof: Since $f$ is semiconjugate to $\sigma$, $\Lambda$ has at least as many components as $\Sigma$. If we can show that for any two distinct points $P$ and $Q$ in $\Lambda$ where $S(P) \neq S(Q)$, the corresponding points in $\Lambda$ are in disconnected components, then the statement is proved automatically.

Suppose $s = (s_0 s_1 \dots) \in \Sigma$ and $t = (t_0 t_1 \dots) \in \Sigma$ are distinct and P, Q are two points in $\Lambda$ that $S(P) = s$ and $S(Q) = t$. Then $s$ and $t$ have to have at least one different digit, say $s_i \neq t_i$. This implies that $f^i(P) \in R_{s_i}$ and $f^i(Q) \in R_{t_i}$ are in different regions (different regions are disconnected due to the escaping axes). Based on the fact that the image of a connected set under a continuous map is also connected, if $P$ and $Q$ were in the same component, then $f^i(P)$ and $f^i(Q)$ would be in the same component. So $P$ and $Q$ are in different components. Therefore, $K(f)$ has at least as many components as the points in $\Sigma$. And because $\Sigma$ has uncountable points, $K(f)$ has uncountable components.

## 3.7 Conjectures

Apparently, the above analysis is just a small part of the dynamical behaviors of $f(z)$. To fully understand this system, we should work more on other cases, especially those which have a profound connection with the distribution of the critical set. Therefore, this section discusses the conjectures that we believe by solving them, we would probably be able to reveal this relationship. These conjectures also serve as the future directions of this research.

### 3.7.1 All Escape Quadrichotomy

For the iteration family $f_{\beta,t}(z) = z^2 + t\frac{\beta}{z^2} + (1-t)\frac{\beta}{\bar{z}^2}$, it seems that $K(f)$ has four cases when the $C(f)$ all escape.

**Theorem.** *If all critical points $C(f)$ lies in $B(\infty)$ and the critical set $C(f)$ consists of four mutually disjoint components, then $K(f)$ has infinitely many components*

We have proved a stronger version of this theorem in section 3.6.2. Figure 3.4(e) shows this case.

**Conjecture.** *If all critical points $C(f)$ lie in $B(\infty)$ and the critical set $C(f)$ consists of one simply closed curve, then $K(f)$ is empty*

Figure 3.4(a) shows this case.

**Conjecture.** *If all critical value set $V(f)$ lie in the trap door and the critical set $C(f)$ consists of one simply closed curve, then $K(f)$ is a Cantor set of circles*

**Conjecture.** *If all critical points $C(f)$ lies in other preimages of $B(\infty)$, then $K(f)$ is a Sierpinski carpet*

### 3.7.2 All Stay Bounded Dichotomy

It seems that there are only two cases when the $C(f)$ all stay bounded.

**Conjecture.** *if the critical set $C(f)$ all stay bounded and consists of mutually disjoint components, then $K(f)$ is a connnected quasi Sierpinski carpet*

Figure 3.3(e) shows this case.

**Conjecture.** *if the critical set $C(f)$ all stay bounded and consists of one simply closed curve, then $K(f)$ is an annulus*

Figure 3.3(b) shows this case.

# Chapter 4

# Conclusion and Discussion

In this paper, we investigated a special map that can connect the nonanalytic and the analytic singular perturbations of the quadratic map. The research shows that this map has a much more complicated dynamical behavior than the two end point cases.

At first, the critical set is no longer separate points as long as the quadratic map is perturbed by a nonanalytic term. Instead, each of these separate points evolves into a closed curve. Then these separate curves merge into one simply closed curve at $t = 0.5$. During this transition, the critical image set also goes from two separate triangles to one closed curve with four swallow tails at the very start. These swallow tails then disappear at $T_b = 2\sqrt{3} - 3$.

Secondly, the parameter plane cannot be subdivided into only four or three regions as shown in Devaney's and Bozyk's studies. There appear to be more intermediate cases:

1. As $t$ varies from 0 to 1, the McMullen Domain disappears at $t = 0.5$.

2. As $t$ varies from 0 to 1, the black strip in figure 3.5(a) shrinks and generates the structure in figure 3.5(f) which was identified by Devaney.

3. As $t$ varies from 0 to 1, the region whose corresponding filled Julia set is empty becomes a region with a nonempty filled Julia set. This nonempty set becomes the Cantor set when $t = 1$.

For each of these transitions in parameter space, the corresponding dynamic plane has even more complicated intermediate cases. We identified two of these special cases: the connected one whose filled Julia set is connected and a disconnected case where the filled Julia set is disconnected. The connected case shows that the appearence of the escape blobs inside the annulus is from the intersection between the critical image set and the boundary of the trap door. The disconnected case is presented by a series of statements that claim the filled Julia set consists of infinitely many components and is no longer a Cantor set for some special parameter combinations $(t, \beta)$. This paper also pointed out that $f$ is semiconjugate to the four symbols shift map for the disconnected case. This semiconjugacy provides a way to understand most of the dynamical behaviors for the nonescape points.

Finally, based on the numerical experiments and analysis, we presented two sets of conjectures: the bounded critical orbits and the escape critical orbits. Note that both of them are very special cases. There are more cases that we cannot even get a conjecture. We hope these conjectures could serve as the directions for our future study.

# References

[1] Daniel Alexander and Robert L Devaney. *A Century of Complex Dynamics*, pages 15–34. Mathematical Association of America, 1 edition, 2015.

[2] Alan F Beardon. *Iteration of Rational Functions*. Springer, 1991.

[3] B.B. Mandelbrot. *The Fractal Geometry of Nature*. Henry Holt and Company, 1982.

[4] J. Milnor. *Dynamics in One Complex Variable*. Annals of Mathematics Studies. Princeton University Press, 2011.

[5] Robert L. Devaney, Krešimir Josić, and Yakov Shapiro. Singular perturbations of quadratic maps. *International Journal of Bifurcation and Chaos*, 14(01):161–169, 2004.

[6] Robert L Devaney. Singular perturbations of complex analytic dynamical systems. *Bulletin of the AMS*, 50:391–429, Jul 2013.

[7] Paul Blanchard, Robert L. Devaney, Daniel M. Look, Pradipta Seal, and Yakov Shapiro. Sierpinski-curve julia sets and singular perturbations of complex polynomials. *Ergodic Theory and Dynamical Systems*, 25(4):10471055, 2005.

[8] Robert L. Devaney and Daniel M. Look. Symbolic dynamics for a sierpinski curve julia set. *Journal of Difference Equations and Applications*, 11(7):581–596, 2005.

[9] Robert L. Devaney and Daniel M. Look. A criterion for sierpinski curve julia sets. *Topology Proceedings*, 30:163–179, 2006.

[10] Robert L. Devaney. Structure of the McMullen domain in the parameter planes for rational maps. *Fundamenta Mathematicae*, 185:267–285, 2005.

[11] Daniel M. Look Robert L. Devaney and David Uminsky. The escape trichotomy for singularly perturbed rational maps. *Indiana Univ. Math. J.*, 54:1621–1634, 2005.

[12] Bruce B Peckham. Real perturbation of complex analytic families: Points to regions. *International Journal of Bifurcation and Chaos*, 08(01):73–93, 1998.

[13] Stefanie Hittmeyer, Bernd Krauskopf, and Hinke M. Osinga. Interactions of the julia set with critical and (un)stable sets in an angle-doubling map on $\mathbb{C}\backslash\{0\}$. *International Journal of Bifurcation and Chaos*, 25(04):1530013, 2015.

[14] Brett Bozyk and Bruce B Peckham. Dynamics of nonholomorphic singular continuations: A case in radial symmetry. *International Journal of Bifurcation and Chaos*, 23, Nov 2013.

[15] Robert L Devaney. Dynamics of $z^n + \lambda/z^n$, why the case $n = 2$ is crazy. *Conformal Dynamics and Hyperbolic Geometry, Contemporary Math*, 573:49–65, 2012.

[16] R.L. Devaney. *A First Course In Chaotic Dynamical Systems: Theory And Experiment*. Studies in Nonlinearity. Avalon Publishing, 1992.

# Appendix A

# Algorithms and Codes

During this research, we used several softwares to do our numerical experiments and generate the figures in this paper. These software includes

1. fraqtive: an open source software by Michał Męciński http://fraqtive.mimec.org/
2. Matlab from MathWorks
3. Mathematica from Wolfram
4. tbc: an open source software by Prof. Bruce Peckham http://www.d.umn.edu/~bpeckham/tbc_home.html

Here are some important codes for the computation in this paper

## A.1 Iteration Function for "Fraqtive"

We modified this software to compute our formula. Therefore, the new iteration algorithm is

```
template<Variant VARIANT>
static inline double calculate( double x, double y, double
   cx, double cy, double exponent, int maxIterations )
{
```

```
//this function calculates if one point on the
   complex plane will escape before the allowed
   iteration time
//the iteration formula is
//f(z)=z\^2+t*beta/(z\^n)+(1-t)beta/(zbar\^n)

//define the local variables
double zx = x;
double zy = y;
double lambda_x=cx;     //parameter beta
double lambda_y=cy;
//double lambda_x=0.001;
//double lambda_y=0;
double power = parameter003;
double t=parameter001;

double radius_z;
double angle_z;
double radius_lambda=pow(pow(lambda_x,2)+pow(
   lambda_y,2),0.5);
double angle_lambda=atan2(lambda_y,lambda_x);

//use polar coordinate to compute next iteration
for ( int k = maxIterations; k > 0; k-- )
{
        adjust<VARIANT>( zx, zy );
        radius_z = pow(pow(zx,2)+pow(zy,2),0.5);

        //if reach the BailoutRadius, then mark this
           point as escape point
        if ( radius_z >= BailoutRadius )
```

```
            return calculateResult( maxIterations, k,
               radius_z, exponent );

            angle_z=atan2(zy,zx);
            zx=pow(radius_z,power)*cos(angle_z*power)+t
               *(radius_lambda/pow(radius_z,power))*cos(
               angle_lambda-power*angle_z)+(1-t)*(
               radius_lambda/pow(radius_z,power))*cos(
               angle_lambda+power*angle_z);
            zy=pow(radius_z,power)*sin(angle_z*power)+t
               *(radius_lambda/pow(radius_z,power))*sin(
               angle_lambda-power*angle_z)+(1-t)*(
               radius_lambda/pow(radius_z,power))*sin(
               angle_lambda+power*angle_z);
      }

      return 0.0;
}
```

This function is in ./src/generatorcore.cpp.

## A.2 Matlab Code to Generate the Filled Julia Set

```
clear all;
t=0.353; %modify t here
beta=0.0625;%modify beta here

%***************generate escape basin****************

%define grid size
M=400;
N=400;
```

```
x=linspace(-1,1,M);
y=linspace(-1,1,N);

%iteration
p=1;
for m=1:M
    for n=1:N
        iter=1;
        rad=sqrt(x(m)^2+y(n)^2);
        zx=x(m);
        zy=y(n);
        while rad<4&&iter<100
            a1=zx^2-zy^2+beta*(zx^2-zy^2)/((zx^2+zy^2)^2);
            a2=2*zx*zy-2*beta*zx*zy*(2*t-1)/((zx^2+zy^2)^2);
            zx=a1;
            zy=a2;
            iter=iter+1;
            rad=sqrt(zx^2+zy^2);
        end
        if iter==100
            pt(p,1)=x(m);
            pt(p,2)=y(n);
            p=p+1;
        end
    end
end

set(gcf,'position',[0,0,820,800]);
plot(pt(:,1),pt(:,2),'.');hold on;

%generate critical set
theta=linspace(0,2*pi,1000);
```

```
radius=abs((beta*(t*cos(4*theta)+sqrt(t^2*(cos(4*theta))
    .^2-2*t+1))).^0.25);
criticalx=radius.*cos(theta);
criticaly=radius.*sin(theta);
plot(criticalx,criticaly);hold on;

%generate image of critical set
for i=1:1000
zx=criticalx(i);
zy=criticaly(i);
criticalimagex(i)=zx^2-zy^2+beta*(zx^2-zy^2)/((zx^2+zy^2)^2)
    ;
criticalimagey(i)=2*zx*zy-2*beta*zx*zy*(2*t-1)/((zx^2+zy^2)
    ^2);
end
plot(criticalimagex,criticalimagey);hold on;

%plot specific points
plot(criticalx(126),criticaly(126),'x');hold on;
plot(criticalimagex(126),criticalimagey(126),'x');hold on;
plot(criticalx(114),criticaly(114),'x');hold on;
plot(criticalimagex(114),criticalimagey(114),'x');hold on;
plot(criticalx(139),criticaly(139),'x');hold on;
plot(criticalimagex(139),criticalimagey(139),'x');hold on;
```

## A.3 Mathematica Code to Compute the $Det(J)(0.5, \beta)$

```
real = x^2 - y^2 + beta (x^2 - y^2)/((x^2 + y^2)^2);
image = 2 x*y - 2 beta*x*y (2 t - 1)/((x^2 + y^2)^2);
J = D[real, x]*D[image, y] - D[real, y]*D[image, x];
J5=J /. {t -> 0.5, x -> 0.5};
```

```
Rs=Solve[(1/4 + y^2)^3 == beta (1/4 - y^2), y];
De=J5/.Rs[[1]]
De/.beta->0.11
De/.beta->0.12
```